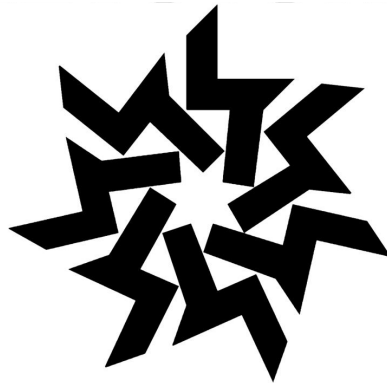


# CEDAR 2017



Keystone Resort, Colorado

**MLT, Coupling, Instrumentation and Techniques  
Poster Session**

Tuesday June 20, 2017

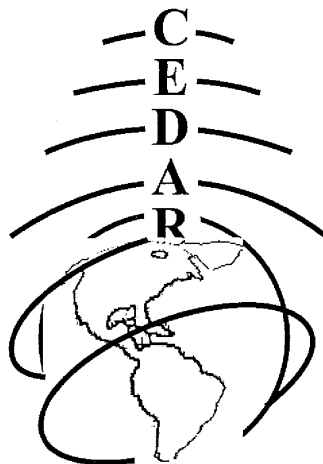


## **Table of Contents**

### **COUPLING OF THE UPPER ATMOSPHERE WITH LOWER ALTITUDES**

<b>COUP-01</b> - Understanding the Non-linear Effects of Eddy Diffusion on the Ionosphere-Thermosphere System - by Garima Malhotra.....	1
<b>COUP-02</b> - Short-term variability in the ionosphere due to the nonlinear interaction between the 6-day wave and migrating tides - by Quan Gan.....	1
<b>COUP-03</b> - Concentric traveling ionosphere disturbances triggered by Super Typhoon Meranti (2016) - by Minyang Chou .....	1
<b>COUP-04</b> - Transitioning a Coupling Whole Atmosphere (WAM) and Ionosphere-Plasmasphere-Electrodynamics (IPE) Model into Operations at NOAA - by Naomi Maruyama .....	2
<b>COUP-05</b> - Investigation of ground level magnetic field disturbances after 2010 Chile 8.8M earthquake - by Pavel Inchin.....	3
<b>COUP-06</b> - Observations and simulations of ionosphere SAO - by Qian Wu.....	3
<b>COUP-07</b> - Longitude dependent lunar tidal modulation of the equatorial electrojet during stratospheric sudden warmings - by Tarique Siddiqui .....	3
<b>COUP-08</b> - Using WACCM-X - by Joe McInerney .....	4
<b>COUP-09</b> - Lower atmospheric gravity waves as sources of low-latitude traveling ionospheric disturbances as studied by an airglow imager, CHAMP satellite, and a general circulation model - by Aysegul Moral .....	4
<b>COUP-10</b> - Investigating the effect of eddy diffusion in mesosphere and lower thermosphere region with multiple data sets - by Chen Wu.....	5
<b>COUP-11</b> - INSPIRESat-1 sampling and observation using the coupled whole atmosphere model and ionosphere model - by Shih-Chi Chiu .....	5

### **IRREGULARITIES OF IONOSPHERE OR ATMOSPHERE**

<b>IRRI-15</b> - Finding multi-scale connectivity in our geospace observational system: Network analysis of total electron content - by Ryan McGranaghan .....	6
--	---

### **INSTRUMENTS OR TECHNIQUES FOR IONOSPHERIC OR THERMOSPHERIC OBSERVATION**

<b>ITIT-01</b> - Expanding Ionospheric Observations with CubeSats: INSPIRESat-1 and IDEASSat - by Loren Chang .....	7
<b>ITIT-02</b> - Recent Progress on Advanced Ionospheric Probe Onboard FORMOSAT-5 Satellite - by Ya-Chih Mao .....	7
<b>ITIT-03</b> - 2-D Energy Flux Maps of Precipitating Electrons using Poker Flat Incoherent Scatter Radar - by Nithin Sivadas.....	7
<b>ITIT-04</b> - Limiting SNR regimes for successful parameter estimation from Retarding Potential Analyzers - by Shantanab Debchoudhury.....	8
<b>ITIT-05</b> - Photochemical model for atomic oxygen ion retrieval from ground-based observations of airglow - by Yi Duann .....	8
<b>ITIT-06</b> - ELF Whistler Dependence on a Sunlit Ionosphere - by Bruce Fritz.....	9
<b>ITIT-07</b> - RENU 2 UV Measurement of Atomic Oxygen in the Cusp Region – by Bruce Fritz.....	9

<b>ITIT-08</b> - Errors in ground-based thermospheric wind and temperature measurements - by Brian Harding .....	<b>9</b>
<b>ITIT-09</b> - Three-dimensional inversion technique for short distance oblique Dynasonde ionograms - by Huan Song .....	<b>10</b>
<b>ITIT-10</b> - Ionospheric Simulations of the 2017 Solar Eclipse QSO Party – by Nathaniel Frissell .....	<b>10</b>
<b>ITIT-11</b> - Coherent scatter from radar aurora: Improvements and applications – by Enrique Rojas Villalba.....	<b>11</b>
<b>ITIT-12</b> - Scientific Measurements Using Software Defined-Radio at MIT Haystack Observatory: Digital RF and it’s Applications - by Bill Rideout .....	<b>11</b>
<b>ITIT-13</b> - Simulation of Particle Flow in Neutral Wind Sensor - by Ellen Robertson.....	<b>11</b>
<b>ITIT-14</b> - The Scintillation Prediction Observations Research Task (SPORT): Anticipated Data Products - by Jim Spann .....	<b>11</b>
<b>ITIT-15</b> - Resolution Metrics for Auroral Multipoint Measurements with Satellite Swarms - by Jonathan Parham.....	<b>12</b>
<b>ITIT-16</b> - Fitting Ionospheric Models Using Real-Time High Frequency Amateur Radio Observations - by Joshua Katz.....	<b>12</b>
<b>ITIT-17</b> - Preliminary Results from LITES and Model Comparison – by George Geddes .....	<b>13</b>
<b>ITIT-18</b> - Particle-in-cell simulations of collisional ISR spectra - by William Longley .....	<b>13</b>
<b>ITIT-19</b> - Thermospheric Measurements With Sounding Rocket Chemical Release Payloads - by Carl Andersen .....	<b>13</b>
<b>ITIT-20</b> - Auroral energy and energy flux derivation using multi-spectral imaging –by Saurav Aryal ..	<b>13</b>
<b>ITIT-21</b> - Geophysical Inversion of thermospheric winds at 250km altitude using higher order Tikhonov regularization on the Alaskan Allsky Fabry-Pert interferometry network for the night of Jan 31st, 2016. - by John Elliott.....	<b>14</b>
<b>ITIT-22</b> - The Design and Function of the Gridded Retarding Ion Distribution Sensor - by Anthony Swenson.....	<b>14</b>
<b>ITIT-23</b> - Investigating Near Space Interaction Regions: Developing a Remote Observatory - by Margaret Gallant.....	<b>15</b>
<b>ITIT-24</b> - Monte-Carlo simulations of ion velocity distributions and resulting incoherent radar spectra under strong ion frictional heating conditions – by Lindsay Goodwin.....	<b>15</b>
<b>ITIT-25</b> - Development of a commercial off-the-shelf software defined radio ionosonde - by Lee Kordella .....	<b>16</b>

**INSTRUMENTS OR TECHNIQUES FOR MIDDLE ATMOSPHERE  
OBSERVATIONS**

<b>ITMA-01</b> - Lower Atmosphere Ionosphere Coupling Experiment - by Channing Philbrick.....	<b>16</b>
<b>ITMA-02</b> - Toward a new capability for upper atmospheric research using atomic oxygen lidar - by James Clemmons .....	<b>16</b>
<b>ITMA-03</b> - LWPC Modeling of Ionospheric Perturbations Due to Lightning Induced Energetic Electron Precipitation Using Overlapping VLF Propagation Paths - by Chad Renick .....	<b>17</b>
<b>ITMA-04</b> - Detection and characterization of Turbulence with Incoherent Scatter Radar - by Jintai Li.	<b>17</b>
<b>ITMA-05</b> - Observability of Acoustic Waves in the MLT by Ground-Based and Airborne Synthetic Airglow Imagers - by Jaime Aguilar Guerrero .....	<b>18</b>

## **LONG-TERM VARIATIONS OF THE MESOSPHERE AND LOWER THERMOSPHERE**

- LTVM-01** - Zonal winds in the tropical middle atmosphere - by Anne Smith .....18
- LTVM-02** - Interannual Variations of SABER CO<sub>2</sub> and CO<sub>2</sub>-based Eddy Diffusion Coefficients in the Mesosphere and Lower Thermosphere Region – by Cornelius Csar Jude Salinas .....19

## **METEOR SCIENCE OTHER THAN WIND OBSERVATIONS**

- METR-01** - A Simulation of Plasma Turbulence from Dust Gradients. - by Matthew Young.....19
- METR-02** - Effect of Plasma Turbulence on the evolution of Specular Meteor Echoes – by Freddy Galindo .....20
- METR-03** - PIC Simulations of 3D Finite Meteor Trails - by Liane Tarnecki .....20

## **MLT GRAVITY WAVES**

- MLTG-01** - Selection of an atmospheric reference model and branching ratios for numerical modeling of gravity wave-airglow interactions - by Yolian Amaro-Rivera .....20
- MLTG-02** - Application of the Transfer Function Model (TFM) in gravity wave modeling - by Robert Bruntz .....21
- MLTG-03** - Measurements of phase differences between temperature and vertical wind perturbations associated with gravity waves in the mesopause region - by Anthony Caton .....21
- MLTG-04** - Multi-Scale Gravity Wave Environments and Influences on Gravity Wave Propagation - by Katrina Bossert .....21
- MLTG-05** - GPS TEC Detection of MSTIDs/LSTIDs and Source Determination – by Ross Dinsmore 22
- MLTG-06** - Classifying mesospheric mountain wave characteristics over New Zealand during the 2014 DEEPWAVE campaign – by Pattilyn McLaughlin.....22
- MLTG-07** - Multi-Year Survey of Short Period Gravity Wave Parameters in the Mesosphere and Lower Thermosphere at McMurdo (77.8°S, 166.7°E), Antarctica - by Ian Geraghty .....23
- MLTG-08** - Automated estimation of dominant horizontal wave parameters appearing in airglow images - by Matthew Grawe .....23
- MLTG-09** - Rayleigh/Raman lidar observations of gravity wave activity in the middle atmosphere over Syowa (69°S, 40°E), Antarctic – by Masaru Kogure .....23
- MLTG-10** - Coupling by gravity waves through the middle and upper atmosphere in Antarctica: Are dominant stratospheric gravity waves the direct source of persistent gravity waves in the MLT? - by Jian Zhao.....24

## **MLTL LIDAR STUDIES**

- MLTL-01** - Investigation of Na layer by numeric simulation - by Xuguang Cai .....25
- MLTL-02** - Depletion of mesospheric sodium during extended period of pulsating aurora: high speed sodium lidar observation - by Toru Takahashi .....25
- MLTL-03** - Simultaneous Lidar Measurements of Fe and Na layers, Temperatures, and Winds in the Mesosphere and Lower Thermosphere-Extended (MLT-X) at Boulder, Colorado - by Dongming Chang .....26
- MLTL-04** - Na lidar measurements of turbulence heat flux, thermal diffusivity and energy dissipation rate in the mesopause region - by Yafang Guo .....26
- MLTL-05** - Initial Results of Na Lidar Measured Stratospheric Temperatures at Andes Lidar Observatory (30.3°S, 70.7°W) - by Shuai Qiao .....26

## **MESOSPHERE OR LOWER THERMOSPHERE GENERAL STUDIES**

<b>MLTS-01</b> - Statistical Characteristics of Short-term Tidal Variability for DW1 in eCMAM30 and SABER - by Ashan Vitharana .....	27
<b>MLTS-02</b> - Validation of NASA TIMED/SABER v2.0 temperature data with ground-based lidars: first results. - by Erin Dawkins .....	27
<b>MLTS-03</b> - Nonlinear acoustic wave effects on lower thermosphere composition - by Benedict Pineyro .....	28
<b>MLTS-04</b> - Mesospheric temperatures during day and night estimated from meteor radar observation - by Jeong-Han Kim.....	29
<b>MLTS-05</b> - Seasonal Variation of Ozone in the Upper Mesosphere at High Latitudes - by Nabil Nowak .....	29
<b>MLTS-06</b> - New method of estimating temperatures near the mesopause region using meteor radar observations - by Changsup Lee.....	29
<b>MLTS-07</b> - Comparison Between Thermospheric Nitric Oxide Emission Observations and the Global Ionosphere-Thermosphere Model (GITM) Simulations: Sensitivity Study to Solar and Geomagnetic Activities - by Cissi Lin.....	30
<b>MLTS-08</b> - Simulations of MLT dynamics with global circulation models and their comparison with mid- and high-latitude ground-based radar observations - by Dimitry Pokhotelov .....	30
<b>MLTS-09</b> - New non-LTE model of OH(v) in the mesosphere/lower thermosphere - by Peter Panka ...	30
<b>MLTS-10</b> - OPAL CubeSatellite Data Analysis Model - by Kenneth Zia.....	31

## **MLTT OTHER TIDAL, PWS, OR SSWS**

<b>MLTT-01</b> - Seasonal and solar cycle variability of DE2 and DE3 in the CO2 15 $\mu$ m cooling of the lower thermosphere - by Nirmal Nischal.....	31
<b>MLTT-02</b> - Exploring Wave-Wave Interactions in a General Circulation Model - by Virginia Nystrom .....	32
<b>MLTT-03</b> - The quasi 2 day wave response in TIME-GCM nudged with NOGAPS-ALPHA - by Jack Wang.....	32
<b>MLTT-04</b> - A New Approach to Study Short-Term Nonmigrating Tidal Variability using Information Theory and Bayesian Statistics - by Komal Kumari.....	32

## **SPRITES**

<b>SPRT-01</b> - Numerical and analytical studies of corona discharge initiation in air & CO2-rich environment - by Jacob Engle .....	33
<b>SPRT-02</b> - Fractal properties of lightning from high-speed video observations - by Ningyu Liu .....	33

## **STRATOSPHERE STUDIES AND BELOW**

<b>STRB-01</b> - Analysis of Black carbon emissions over a semi-urban station Vijayawada: Preliminary results - by Prasad Perumal.....	34
<b>STRB-02</b> - Carbon dioxide in the polar stratosphere from AIM/SOFIE measurements - by Yucheng Su .....	35

## COUPLING OF THE UPPER ATMOSPHERE WITH LOWER ALTITUDES

### **COUP-01 - Understanding the Non-linear Effects of Eddy Diffusion on the Ionosphere-Thermosphere System - by Garima Malhotra**

Status of First Author: Student IN poster competition PhD

**Authors:** Garima Malhotra, Aaron Ridley

**Abstract:** The thermosphere is one of the most dynamic regions of the Earth's atmosphere because of its coupling with the electromagnetically active ionosphere, magnetosphere and the strong influence of turbulence from neutral dominated lower atmospheric regions (stratosphere and mesosphere). The composition and temperature changes in this region affect the satellites' drag and thus their trajectories. Disruption of satellite systems can wreak havoc on human communication, surveillance and environment. However, the exchange of energy between lower atmospheric regions with the ionosphere thermosphere (IT) system is not well understood. Specifically, we lack the data and methods to understand the spatial and temporal effects of eddy turbulence in the thermosphere. This arises mainly because turbulence due to eddy diffusion cannot be directly measured and that it is a challenge to completely characterize its linear and non-linear effects from other influences. In this study, we analyze the sensitivity of the thermospheric densities, O/N<sub>2</sub> ratio, temperature, TEC to the turbulence from the lower atmosphere by understanding the nature of eddy diffusion, turbulence and heat transport in Global Ionosphere Thermosphere Model (GITM). We also impose a seasonal and latitudinal variation to the eddy diffusion coefficient using the measurements from MSIS to bring the densities closer to the CHAMP and GRACE densities, and TEC closer to GPS values. We also impose a linear trend of 15% per decade which further improves the agreement between GITM output and thermospheric observational data.

### **COUP-02 - Short-term variability in the ionosphere due to the nonlinear interaction between the 6-day wave and migrating tides - by Quan Gan**

Status of First Author: Non-student PhD

**Authors:** Jens Oberheide; Jia Yue; and Wenbin Wang

**Abstract:** Using the Thermosphere-Ionosphere-Mesosphere Electrodynamics General Circulation Model simulations, we investigate the short-term ionospheric variability due to the child waves and altered tides produced by the nonlinear interaction between the 6-day wave and migrating tides. Via the Fourier spectral diagnostics and least-square fittings, the [21hr, W2] and [13hr, W1] child waves, generated by the interaction of the 6-day wave with the DW1 and SW2, respectively, are found to play the leading roles on the sub-diurnal variability (e.g., 10 m/s in the ion drift and ~ 50% in the NmF2) in the F-region vertical ion drift changes through the E-region dynamo modulation. The relatively minor contribution of the [11hr, W3] child wave is explicit as well. Although the [29hr, W0] child wave has the largest magnitude in the E-region, its effect is totally absent in the vertical ion drift due to the zonally uniform structure. But, the [29hr, W0] child wave shows up in the NmF2. It is found that the NmF2 short-term variability is attributed to the wave modulations on both the E-region dynamo and in-situ F-region composition. Also, the altered migrating tides due to the interaction will not contribute to the ionospheric changes significantly.

### **COUP-03 - Concentric traveling ionosphere disturbances triggered by Super Typhoon Meranti (2016) - by MINYANG CHOU**

Status of First Author: Student IN poster competition PhD

**Authors:** M. Y. Chou, C. H. Lin, Jia Yue, H. F. Tsai, Y. Y. Sun, J. Y. Liu, and C. H. Chen

**Abstract:** Concentric traveling ionosphere disturbances (CTIDs) in total electron content triggered by Super Typhoon Meranti on 13 September 2016 are detected by using the ground-based Global Navigation Satellite Systems network in Taiwan. The CTIDs emanated outward before the typhoon landfall and lasted for more than 10 h. The characteristics of CTIDs agree with the gravity wave theory and exhibit spatial and temporal scales in wave periods of ~8–30 min, horizontal wavelengths of ~160–200 km, and horizontal phase velocities of ~106–220 m/s. We also observe the CTIDs showing the stationary wave character. Broad spectra of CTIDs are excited after the rainbands of typhoon impinged on Central Mountain Range of Taiwan. The ray-tracing technique confirms that the CTIDs were excited by convective clouds, spiral rainbands, and the eyewall of Typhoon Meranti. This study provides new evidence of typhoon-induced concentric gravity waves in the ionosphere.

## **COUP-04 - Transitioning a Coupling Whole Atmosphere (WAM) and Ionosphere-Plasmasphere-Electrodynamics (IPE) Model into Operations at NOAA - by Naomi Maruyama**

Status of First Author: Non-student PhD

**Authors:** Naomi Maruyama, Tim Fuller-Rowell, Rashid Akmaev, Rodney Viereck, Tzu-Wei Fang, Mariangel Fedrizzi, Mihail Codrescu, Valery Yudin, Zhuxiao Li, Phil Richards, George Millward, Robert Oehmke, Cecelia DeLuca, Weiyu Yang, Mark Iredell, Jacques Middlecoff, and Mark Govett

**Abstract:** In an effort to model the space weather system from the Sun to Earth, NOAA is transitioning three separate physical model components. These include the WSA-ENLIL solar wind propagation model, the Michigan Geospace model of the magnetosphere, and a coupled model of the whole atmosphere and the ionosphere-plasmasphere-electrodynamics (WAM-IPE). The first two of these components have already been transitioned to operations at NOAA, and the third component is due to be tested in an operational real-time setting in September 2017. WAM is a whole atmosphere extension of the National Weather Service (NWS) Global Forecast System (GFS) operational weather model, extending the top boundary from 60 km in GFS to ~600 km in WAM. WAM can also be run with the NWS Gridpoint Statistical Interpolation (GSI) data assimilation scheme in order for WAM to follow real changes in tropospheric weather. The WAM model is coupled to a new Ionosphere-Plasmasphere-Electrodynamics (IPE) model, using the Earth System Modeling Framework (ESMF) and the National Unified Operational Prediction Capability (NUOPC) layer, under the NOAA Environmental Modeling System (NEMS). IPE is a time dependent, three-dimensional model of the ionosphere and plasmasphere developed through a collaboration between University of Colorado, George Mason University, NOAA Space Weather Prediction Center (SWPC), NOAA Global Systems Division (GSD), NCAR HAO, and NESII. WAM provides the thermospheric properties of wind, composition, and temperature to the IPE, and can respond to changes in terrestrial weather propagating upward and influencing the thermosphere. IPE in turn provides time dependent, global, three-dimensional plasma densities for nine ion species, electron and ion temperatures, and both parallel and perpendicular velocities of the ionosphere and plasmasphere. IPE reproduces not only the climatology of global TEC observations, but the model also responds to changes in solar wind conditions during geomagnetic storms, and to terrestrial lower atmosphere changes, such as during sudden stratospheric warmings (SSW). The model follows the storm time redistribution of plasma in the ionosphere and plasmasphere during an SSW, and the evolution of storm enhanced densities (SEDs) during a geomagnetic storm. In this presentation, an overview of the WAM and IPE model development and current status is presented. Furthermore, the configuration expected to be transitioned in September will be described. It is important to establish this baseline configuration, which will gradually be improved over the coming years. In the future, the WDAS data assimilation in the lower atmosphere will be extended into the thermosphere and ionosphere to better address operational needs.

## **COUP-05 - Investigation of ground level magnetic field disturbances after 2010 Chile 8.8M earthquake - by Pavel Inchin**

Status of First Author: Student IN poster competition Masters

**Authors:** P.A. Inchin, M.D. Zettergren, J.B. Snively, A. Komjathy, and O. Verkhoglyadova

**Abstract:** Recent scientific reports have identified geomagnetic field perturbations likely due to acoustic and gravity wave-driven ionospheric dynamo phenomena following natural hazard events [e.g. Aoyama et al, EPS(68:148) 2016; Toh et al, JGR(116) 2011]. Particularly, the connection between acoustic wave-generated currents to magnetic perturbations were found after several severe earthquakes [Iyemori et al, EPS(65:901) 2013; Hasbi et al, ASTP(71) 2005]. Moreover, modeling results showed good similarity with observed fluctuations of the geomagnetic field at the ground level [Zettergren and Snively, JGR(120) 2015].

Here, we report model-data comparisons of results based on Zettergren and Snively [2015] and analyses of ground level magnetic field perturbations following the 2010 Chile 8.8M earthquake. Iyemori et al. [2013] presented comparisons of barometric and magnetic data following this earthquake; they interpreted long-period magnetic oscillations (with main peaks at ~190 and 265 sec) as the effect of field-aligned current generated through a dynamo process in the ionosphere. In our study, we perform complementary spatial and temporal analyses of the disturbances in ionospheric electron density and in magnetic field. Integrated ionospheric total electron content (TEC) data from regional ground-based GNSS receivers and magnetic field data from SAMBA magnetometers network are analyzed. Data from regional networks of seismometers are also utilized to discern magnetic field perturbations caused by surface waves and by acoustic wave-generated currents to the ground. Results suggest that frequencies of perturbations of magnetic field (~4-5 mHz) on ground level appear close to those observed in TEC data, which supports the hypothesis made in Iyemori et al. [2013] that they are due to acoustic wave-generated currents.

## **COUP-06 - Observations and simulations of ionosphere SAO - by Qian Wu**

Status of First Author: Non-student PhD

**Authors:** W. S. Schreiner, S.-P. Ho, H.-L. Liu, and Liying Qian

**Abstract:** It is known that the ionosphere has strong semiannual oscillation (SAO). We use the NCAR TIEGCM (Thermosphere Ionosphere Electrodynamics General Circulation Model) model to investigate the eddy diffusion and tidal effects on the ionosphere SAO. We also use the COSMIC (Constellation Observing System for Meteorology, Ionosphere, and Climate) satellite GPS radio occultation (RO) observations to valid the simulation results. The TIEGCM is driven at 97 km lower boundary by tidal and gravity wave (eddy diffusion coefficient) inputs. Adding SAO to the eddy diffusion coefficient at the TIEGCM lower boundary enhances the simulated ionosphere SAO and agrees well with the COSMIC observations. Removing the tides at the lower boundary makes the modeled ionosphere density and SAO too large compared to the COSMIC observation. The TIEGCM simulations are consistent with the diurnal signal in the ionosphere density being mostly in-situ existed and semidiurnal from lower atmosphere. Consequently, the diurnal signal is more affected by the eddy diffusion related electron density SAO than the semidiurnal variation.

## **COUP-07 - Longitude dependent lunar tidal modulation of the equatorial electrojet during stratospheric sudden warmings - by Tarique Siddiqui**

Status of First Author: Student IN poster competition Masters

**Authors:** Dr. Claudia Stolle, Dr. Hermann Lühr



**Abstract:** The ionosphere, in addition to being under solar control, is also affected by meteorological processes that occur in the troposphere and stratosphere. An example of this vertical coupling can be seen during a stratospheric sudden warming (SSW) event. The atmospheric phenomenon of SSW is confined to the winter polar stratosphere but its influence can even be seen at the equatorial and low latitude ionosphere. The connection between the polar stratosphere and the equatorial ionosphere during SSWs is mainly believed to be through the modulation of global atmospheric tides that are known to influence the electrical dynamo process responsible for the generation of electric fields and currents in the ionosphere. Observational evidence in the ionosphere suggest that in response to the SSWs, the amplitude of the lunar semidiurnal tide shows a large enhancement thereby becoming an important driver of the ionospheric variability during SSWs. It is believed that the change in the middle atmosphere due to SSW induced variabilities lead to the lunar tidal amplification in the mesosphere-lower thermosphere (MLT) and in the ionosphere.

In this study, we report about the longitudinal variabilities in lunitidal enhancement in the equatorial electrojet (EEJ) during SSWs through ground and space observations in the Peruvian and Indian sectors. We observe that the amplification of lunitidal oscillations in EEJ is significantly larger over the Peruvian sector in comparison to the Indian sector. We further compare the lunitidal oscillations in both the sectors during the 2005-2006 and 2008-2009 major SSW events and during a non-SSW winter of 2006-2007. It is found that the lunitidal amplitude in EEJ over the Peruvian sector showed similar enhancements during both the major SSWs but the enhancements were notably different in the Indian sector. Independent from SSW events, we have also performed a climatological analysis of the lunar modulation of the EEJ during December solstice over both the sectors by using 10 years of CHAMP magnetic measurements and found larger lunitidal amplitudes over the Peruvian sector confirming the results from ground-magnetometer observations. We have also analysed the semidiurnal lunar tidal amplitude in neutral temperature measurements from SABER at 110 km and found lesser longitudinal variability than the lunitidal amplitude in EEJ. Our results suggest that the longitudinal variabilities in the lunitidal modulation of the EEJ during SSWs could be related to electrodynamics in the E-region dynamo. The stratosphere-ionosphere coupling during SSW events provides an opportunity to better understand the processes behind the lower atmospheric forcing of the ionosphere and to improve capabilities that may in future lead to ionospheric weather forecasting.

### **COUP-08 - Using WACCM-X - by Joe McInerney**

Status of First Author: Non-student

**Authors:** Joe McInerney

**Abstract:** The next release of the Community Earth System Model (CESM) is scheduled for the summer of 2017 and will include a functional version of the Whole Atmosphere Community Climate Model - eXtended (WACCM-X) with a more thorough ionosphere and thermosphere. The WACCM-X model is being developed at the National Center for Atmospheric Research (NCAR) High Altitude Observatory (HAO) in Boulder, Colorado and is based on the Whole Atmosphere Community Climate Model (WACCM) and the Community Atmosphere Model (CAM), both part of the atmospheric component of CESM. While CAM extends from the ground to ~30km and WACCM to ~140km, WACCM-X has a model top of ~600km. Here we give an overview of features included in this upcoming WACCM-X release, including improvements based on the heritage of the Thermosphere Ionosphere Electrodynamics - General Circulation Model (TIE-GCM). We also present future short-term and long-term developments.

### **COUP-09 - Lower atmospheric gravity waves as sources of low-latitude traveling ionospheric disturbances as studied by an airglow imager, CHAMP satellite, and a general circulation model - by Aysegul Moral**

Status of First Author: Student IN poster competition PhD

**Authors:** A.C. Moral, K. Shiokawa, H. Liu, Y. Otsuka, S. Suzuki, C. Yatini and E. Yigit

**Abstract:** Traveling ionospheric disturbances (TIDs) are studied by using three CHAMP satellite overpasses on ground-based 630-nm airglow images at low-latitudes. The airglow images are obtained from Kototabang (KTB), Indonesia (geographic coordinates: 0.2S, 100.3E, geomagnetic latitude: 10.6S). Three TID events that were simultaneously measured by the imager and CHAMP are selected for further investigation: April 30, 2006 (event 1), September 28, 2006 (event 2) and April 12, 2004 (event 3). All events show southward-moving structures in airglow images. The events 1 and 2 are single pulse events with horizontal scales of ~500-1000 km and event 3 show five wavefronts with horizontal scale sizes of 500-1000 km. For events 1 and 3, the neutral density in CHAMP shows out-of-phase variations with the airglow intensity, while event 2 is in-phase. For event 1, the relation between electron density and airglow intensity is out of phase, while the relationship between electron density and airglow intensity enhancement of event 2 and 3 are unclear, which implies that ionospheric plasma variation is not the cause of the observed TIDs. If gravity waves in the thermosphere are the source of the observed TIDs, in-phase and out-of-phase relationships of neutral density and airglow intensity can be explained by different vertical wavelengths of the gravity wave. We estimate possible vertical wavelengths for those events using observed wave parameters and modeled neutral winds. Finally, we further study the event 1 by using a general circulation model that incorporates the whole atmosphere nonlinear gravity wave scheme of Yiğit et al. (2008) and demonstrate that direct gravity propagation from the lower atmosphere to thermosphere can appreciably contribute to the observed airglow intensity enhancements. Based on these investigations, we conclude that internal gravity waves are the cause of the observed TIDs.

### **COUP-10 - Investigating the effect of eddy diffusion in mesosphere and lower thermosphere region with multiple data sets - by Chen Wu**

Status of First Author: Student NOT in poster competition PhD

**Authors:** Chen Wu, Aaron Ridley, and Gang Chen

**Abstract:** Eddy diffusion in mesosphere and lower thermosphere region plays a crucial role in models of upper atmosphere, for its effect on the distribution of thermospheric composition and thermodynamics and the subsequent effects on the chemistry and dynamics of thermosphere and ionosphere. While it is difficult to directly model the sub-grid-scale mixing, multiple parameters are chosen to simulate the effect of eddy diffusion. In order to determine how to set the parameters within the model correctly, analysis was conducted on multiple data sets. The analysis of CO<sub>2</sub> data from the Sounding of the Atmosphere using Broadband Emission Radiometry (SABER) shows that the effect region of eddy diffusion varied with latitudes, seasons, and year. The region of competition between eddy diffusion and molecular diffusion is about 0.001-0.01 mbar, while the Global Ionosphere Thermosphere Model (GITM) typically sets the pressure level in which the eddy diffusion starts to decrease at 0.001, which may be too low of a pressure. The O/N<sub>2</sub> ratio obtained from the Global Ultraviolet Imager (GUVI) provides the volume emission rate below the satellite, which roughly provides global coverage over a day. Comparisons with the simulation results of the GITM show that the simulations are ~2 times as large as the observations, which indicates that the eddy diffusion is likely to be underestimated. Finally, Eddy diffusion can affect the ionosphere, due to the uplifting/down welling of the molecular rich air. In terms of the daily foF<sub>2</sub>, hmF<sub>2</sub>, TEC, etc., the model and the data agree rather well, despite the clear difference in O/N<sub>2</sub> ratio. This poster will explore each of these different effects and summarize the research that has been conducted so far.

### **COUP-11 - INSPIRESat-1 sampling and observation using the coupled whole atmosphere model and ionosphere model - by Shih-Chi Chiu**

Status of First Author: Student IN poster competition Masters

**Authors:** Shih-Chi Chiu, Loren Chang, Tzu-Wei Fang, Amal Chandran, Jack Wang, Pei-Yun Chiu, Yi Duann, Rong Tsai-Lin, and Wei-Hao Luo

**Abstract:** "The International Satellite Program in Research and Education (INSPIRE) is an international collaboration for CubeSat development and for Earth and space science research, which consists of National Central University (NCU) in Taiwan, University of Colorado at Boulder (CU) in U.S., and the Indian Institute of Space Science and Technology (IIST) in India. INSPIRESat-1 is the first CubeSat mission of this program, which will use the Compact Ionosphere Probe (CIP) as its payload, and is expected to be launched in 2019. CIP has the ability to measure ionospheric parameters in situ, including ion and electron temperature, ion velocity, electron density, and ion composition.

Two science objectives of INSPIRESat-1 are observing the Equatorial Plasma Irregularities (EPIs) and measuring the ion temperature to infer the Midnight Temperature Maximum (MTM). To achieve the scientific objectives and to complement the upcoming two low-latitude missions, FORMOSat-7/COSMIC-2 and the NASA Ionospheric Connection Explorer (ICON), the higher inclination orbits are considered for INSPIRESat-1. In this poster, we sample the electron density and ion temperature from simulations of the coupled Whole Atmosphere Model (WAM) and Global Ionosphere and Plasmasphere Model (GIP) to demonstrate the variations of these parameters with inclinations between 20° to 70° and the altitudes from 400 to 600 kilometers. We also consider the effects of these different orbits with regard to constraints on mission lifetime and downlink data volume, as well as the relation to current and upcoming missions carrying similar in-situ plasma sensors. This exercise helps to identify the most suitable orbit for INSPIRESat-1. We expect the comprehensive ionospheric measurements taken by INSPIRESat-1 will provide better insights into the physics of EPIs and MTM."

## IRREGULARITIES OF IONOSPHERE OR ATMOSPHERE

### **IRRI-15 - Finding multi-scale connectivity in our geospace observational system: Network analysis of total electron content - by Ryan McGranaghan**

Status of First Author: Non-student PhD

**Authors:** Anthony J. Mannucci, Olga Verkhoglyadova, and Nishant Malik

**Abstract:** System science has emerged as a promising approach to understanding, and ultimately predicting, the complex, coupled magnetosphere-ionosphere-thermosphere (MIT) environment. Total electron content (TEC) data obtained from Global Navigation Satellite System (GNSS) signals is one of the most valuable datasets available to study the systems-level (global) MIT environment. However, to gain the most utility from these data new, data-driven, approaches are needed.

We present the first complex network theory-based analysis of high-latitude TEC data, including dependencies on interplanetary magnetic field (IMF) clock angle and hemisphere. We examine several network measures to quantify the spatio-temporal correlation patterns in the TEC data for winter and summer months in 2016. We find that significant structure exists in the correlation patterns, distinguishing the dayside and nightside ionosphere, and specific features in the high latitudes such as the polar cap and auroral oval, including the cusp and ionospheric footpoints of magnetospheric boundary layers. These features vary with the IMF, exhibiting a strong dependence on the north-south direction and generally larger variations during the winter months in both hemispheres. Our exploratory results suggest that network analysis of TEC data can be used to study characteristic ionospheric spatial scales at high-latitudes, thereby extending the utility of these data. Together with an identification of important areas of future work, our findings provide a foundation for the application of network analysis techniques to ionospheric TEC. Our results suggest that network analysis can reveal new physical connections in the ionospheric system.

## INSTRUMENTS OR TECHNIQUES FOR IONOSPHERIC OR THERMOSPHERIC OBSERVATION

### **ITIT-01 - Expanding Ionospheric Observations with CubeSats: INSPIRESat-1 and IDEASSat - by Loren Chang**

Status of First Author: Non-student PhD

**Authors:** Loren C. Chang, Chi-Kuang Chao, Amal Chandran, Tzu-Wei Fang, Charles C.H. Lin, Tiger J.Y. Liu, Cornelius Jude H. Salinas, Ya-Chih Mao, Pei-Yun Chiu, Jack Wang, Yi Duann, Rong Tsai-Lin, Shih-Chi Chiu, and Wei-Hao Luo

**Abstract:** In-situ observations of ionospheric plasma densities, temperatures, composition, and drift velocities play an important role in understanding the spatial structure and variability of the ionosphere, as well as the vertical coupling mechanisms linking the thermosphere/ionosphere system to the Sun, geospace, and lower atmosphere. Satellites are a valuable platform for global scale observations of the aforementioned phenomena, but can be limited in terms of local time and latitude coverage. Constellations of small satellites have the potential to greatly expand our observational capability. We present an overview of two funded 3U CubeSat missions under Phase A development - INSPIRESat-1 and IDEASSat, respectively projected for launch in 2019 and 2020. Both spacecraft will carry the Compact Ionosphere Probe - an all in one in-situ sensor with Retarding Potential Analyzer (RPA), Ion Drift Meter (IDM), Ion Trap (IT), and Planar Langmuir Probe (PLP) modes, with heritage from Taiwan's sounding rocket program, as well as FORMOSAT-5. We discuss how these two CubeSats can complement and extend the observations of current and upcoming missions with similar payloads, as well as the challenges and tradeoffs inherent in the design process.

### **ITIT-02 - Recent Progress on Advanced Ionospheric Probe Onboard FORMOSAT-5 Satellite - by Ya-Chih Mao**

Status of First Author: Student NOT in poster competition PhD

**Authors:** Chi-Kuang Chao, Zai-Wun Lin

**Abstract:** Advanced Ionospheric Probe (AIP) is a piggyback science payload developed by National Central University for FORMOSAT-5 satellite since 12 January 2012. The AIP is an all-in-one plasma sensor to measure ionospheric plasma concentrations, velocities, or temperatures in a time-sharing way. Meanwhile, the AIP is capable of measuring ionospheric plasma irregularities with sampling rate up to 8,192 Hz over a wide range of spatial scales. Electroformed gold grids used in the AIP can reduce quasi-hysteresis effect on current-voltage curves in a plasma injection test and approximate ideal electrical potential surfaces for accurate data available in the future. The AIP flight model has passed through preliminary and critical design review, functional and environmental tests, and then was delivered to the NSPO on 8 October 2013. It is scheduled to launch into a low Earth orbit on a Falcon 9 rocket manufactured by Space Exploration Technologies Corp. from Vandenberg Air Force Base in the 2nd quarter 2016 to carry out a two-year scientific mission on space weather and seismic precursors. At the beginning the AIP will be routinely operated within  $\pm 75^\circ$  latitude in the night-side sector to meet a 5-W limit in average power per orbit due to high power consumption and a heat dissipation issue. Up to 1.5 gigabits per day in data storage, the AIP is capable to perform 8,192 electric current readings per second with duty cycle under 10% to resolve fine structure of equatorial ionospheric plasma irregularities within  $\pm 18^\circ$  latitude.

### **ITIT-03 - 2-D Energy Flux Maps of Precipitating Electrons using Poker Flat Incoherent Scatter Radar - by Nithin Sivadas**

Status of First Author: Student IN poster competition Masters

**Authors:** Nithin Sivadas, Toshi Nishimura, and Josh Semeter

**Abstract:** Energetic particle precipitation can cause enhanced conductivity structures that affect current flow in the ionosphere, which in turn can affect magnetospheric convection. Global precipitation models are therefore essential in understanding magnetosphere-ionosphere coupling. However, existing precipitation models are statistical and they do not capture small-scale structural and temporal variations. This drawback hampers accurate modelling of the magnetosphere-ionosphere dynamics during substorms. Quantitative and continuous multi-point measurements of particle precipitation are essential in estimating the small-scale spatial and temporal variations of precipitating particles. For this reason, we have developed a novel technique to estimate energy flux maps of precipitating electrons spanning latitude, longitude, time and energy. The technique inverts electron density measurements from Poker Flat Incoherent Scatter Radar to estimate the primary electron energy flux that caused the ionization. In this poster, we demonstrate the capabilities of the energy flux maps to identify precipitation structures during a large substorm on 26th March 2008. Our observations during the growth phase of the substorm show a clear precipitation of high energy electrons  $\sim 100$  keV associated with the stable trapping boundary. Unlike in-situ and single point measurements, this technique offers continuous diagnostics of precipitating electrons with a spatial coverage of  $\sim 50 \times 50$  km. The ability to quantitatively observe spatial structure and time evolution of energetic precipitation promises to improve our understanding of magnetosphere-ionosphere coupling.

#### **ITIT-04 - Limiting SNR regimes for successful parameter estimation from Retarding Potential Analyzers - by Shantanab Debchoudhury**

Status of First Author: Student NOT in poster competition PhD

**Authors:** Srijan Sengupta, Gregory Earle

**Abstract:** Retarding Potential Analyzers (RPA) are very popular among researchers interested in inferring a large number of ionospheric quantities from space-borne satellites. However, the estimated parameters from RPAs suffer from inaccuracies in the presence of instrument noise. With the miniaturization of cubesats the signal-to-noise ratio (SNR) becomes an increasingly important factor in the performance of an RPA. Least square minimization techniques like Levenberg Marquardt can produce inaccurate estimates of plasma parameters when the SNR is low, and this may occur frequently in low density plasmas. In this project, we look at the low SNR regimes and try to characterize the limiting noise cases beyond which the estimation process is largely dominated by erroneous signals.

#### **ITIT-05 - Photochemical model for atomic oxygen ion retrieval from ground-based observations of airglow - by Yi Duann**

Status of First Author: Student IN poster competition Masters

**Authors:** L. C. Chang, Y. C. Chiu

**Abstract:** To study the chemistry and composition of the upper atmosphere, we can utilize airglow emissions from the photochemical reactions of the ions in this region. When the atomic oxygen ions distributed in the ionospheric F region experience an energy level transition, visible light with a wavelength of 630 nm is released. We used the photometer system built by our team to perform ground-based observations of airglow over the sky of Taiwan at Lulin Observatory ( $23^{\circ}28'07''\text{N}$ ,  $120^{\circ}52'25''\text{E}$ ) during nighttime. We combined the mean values of our observations every 10 minutes with a photo chemistry model based on the formula derived from the theories of R. Link and L. L. Cogger (1988), Sobral et al (1993), and Vladislav Yu. Khomich et al. (2008). With these different methods, we can estimate how the density of oxygen atomic ions varies with time and altitude, and compare the results from empirical models with satellite-based observation data from FORMOSAT-3/COSMIC. This system will be used for long term observations to study the whole year variation of upper atmosphere composition.

Ground-based airglow photometer observations throughout 2016 from the Institute of Solar-Terrestrial Physics (ISTP) in Irkutsk, Russia are also analyzed using these models. The atomic oxygen ion density calculated by our photochemical models show a similar tendency as the ground-based time variation of airglow radiance (Rayleigh) and the electron density observations of FORMOSAT-3/COSMIC. The pattern of atomic oxygen ion variation is resolved by our inversion model, which will be utilized for further analysis of ionospheric composition variation in the future.

### **ITIT-06 - ELF Whistler Dependence on a Sunlit Ionosphere - by Bruce Fritz**

Status of First Author: Student IN in poster competition PhD

**Authors:** Bruce Fritz, Marc Lessard, John Heavisides, Hyomin Kim, and Kaiti Wang

**Abstract:** Whistler-like spectral features in the extremely low frequency (ELF) range have been observed at the South Pole Station. Analysis of the first full year of data reveal a correlation between the occurrence of ELF whistlers and the solar zenith angle (SZA). ELF whistlers stop appearing for the duration of the polar winter, when the SZA increases to greater than 80°. Previous studies at lower geographic latitudes all observed a noon-time peak in the occurrence rate, which led to speculation of source mechanisms in the dayside magnetosphere. The extended polar winter allows for a separation of “dayside” and “sunlit” conditions. The absence of ELF whistlers in the polar winter implies that ELF whistler explicitly depend on local ionospheric conditions.

### **ITIT-07 - RENU 2 UV Measurement of Atomic Oxygen in the Cusp Region – by Bruce Fritz**

Status of First Author: Student NOT poster competition PhD

**Authors:** Bruce Fritz, Marc Lessard, David Kenward, Jim Clemmons, Jim Hecht, Kristina Lynch, David Hysell, Geoff Crowley, Tim Cook, and Supriya Chakrabarti

**Abstract:** The RENU 2 NASA sounding rocket mission launched from the Andoya Space Center on 13 December, 2015 into the dayside cusp region. A UV Photometer (UV PMT) provided by the University of New Hampshire was oriented to look up along the local magnetic field line as the payload passed through a poleward moving auroral form (PMAF). The bandpass filter on the UV PMT isolated emissions of atomic oxygen at both 130.4 nm and 135.6 nm. The instrument measured a clear enhancement in the topside ionosphere as the payload descended through a region of soft electron precipitation. The RENU 2 UV PMT was flown uncalibrated but measured a clear signal with both a major overall structure as well as several smaller peaks of fine structure. An identical spare has been built and calibrated using a Paresce UV light source at UMass-Lowell to compare and correlate with the flight data. An approximation of the flight data luminosity from the spare instrument and other flight data from RENU 2 is used in a radiative transport model to infer structure of upwelling neutral atomic oxygen above the PMAF.

### **ITIT-08 - Errors in ground-based thermospheric wind and temperature measurements - by Brian Harding**

Status of First Author: Student NOT in poster competition PhD

**Authors:** Brian J. Harding, Jonathan J. Makela

**Abstract:** Detector technology has improved to the point where statistical errors in ground-based wind and temperature measurements are now smaller than systematic errors, at least for temporal resolutions of several tens of seconds. As these data are beginning to be used more quantitatively (e.g., in assimilative models), it is becoming increasingly important to accurately estimate these errors, which are caused by

instrument stability, the variability of the airglow peak height and width, hydroxyl emissions, and scattering of airglow radiation in the troposphere. In this work, we quantify and propose community standards for the reporting of these errors, with special focus on scattering, which has not previously been studied during quiet times. We develop a radiative transfer model which suggests that scattering causes ground-based wind measurements to be biased ~10% low on average, while temperatures are biased high by several K. For all of these systematic errors, corrections are possible but introduce significant uncertainty.

### **ITIT-09 - Three-dimensional inversion technique for short distance oblique Dynasonde ionograms - by Huan Song**

Status of First Author: Student IN poster competition PhD

**Authors:** Huan Song; Nikolay Zabotin

**Abstract:** Existing inversion technique for vertical incidence Dynasonde ionograms (NeXtYZ) produces vertical profiles of the electron density and of the two components of the plasma tilts. It proved to be a valuable tool for studies of traveling ionospheric disturbances (TIDs) and associated atmospheric gravity waves (GWs). A generalization of this technique for bi- and multi-static sounding configurations is required, to be used for regional interferometric measurements of GWs. Such generalization is proposed here to obtain the plasma density profile and tilts information at the middle point of an oblique sounding path. Numerical ray tracing technique is used to simulate a list of echoes for an oblique Dynasonde ionogram based on a realistic model of disturbed ionospheric plasma density distribution including TIDs and small-scale irregularities. The inversion procedure involves restoration of parameters of the wedge stratified ionosphere model for the middle point of an oblique sounding path, using multiple ray tracing technique and various optimization methods. The inversion procedure can make full use of both extraordinary and ordinary echoes in the simulated oblique ionogram and takes into account the geomagnetic field. To verify the performance of the proposed method, oblique ionograms were simulated with various parameters of the plasma density model, both with small-scale irregularities and without them. The test results show that the calculated plasma density profile fits well with the real plasma density profile. In addition, the calculated ionospheric tilts profile reproduces accurately the model characteristics when small-scale irregularities are included. Our results confirm feasibility of expansion of the standard vertical operation of Dynasonde systems to bi- and multi-static sounding modes.

### **ITIT-10 - Ionospheric Simulations of the 2017 Solar Eclipse QSO Party – by Nathaniel Frissell**

Status of First Author: Non-student PhD

**Authors:** N. A. Frissell, J. Katz, G. D. Earle, M. L. Moses, E. S. Miller, A. J. Gerrard, and M. L. West

**Abstract:** On August 21, 2017 a total solar eclipse will traverse the continental United States from Oregon to South Carolina. In addition to their stunning visual display, solar eclipses are known to have a significant impact on the ionosphere. This is due to the moon's shadow causing a relatively abrupt cessation of photoionization that can lead to a decrease in D, E, and F region ionospheric densities. In spite of years of research, the spatial and temporal scales of eclipse ionospheric effects are not well known. This is due to eclipses being relatively rare events as well as only a recent availability of instrumentation capable of instantaneous continental-scale ionospheric imaging. To address these questions, amateur (ham) radio operators will take part in the 2017 Solar Eclipse QSO Party, a citizen science experiment in which ham radio operators will illuminate the ionosphere over the continental United States using HF signals in order to remotely sense the ionosphere. We present simulations of this event using the PHARLaP toolkit to raytrace signals from between a realistic set of transmitters and receivers through a numerical model of the eclipsed ionosphere.

## **ITIT-11 - Coherent scatter from radar aurora: Improvements and applications – by Enrique Rojas Villalba**

Status of First Author: Student IN poster competition Masters

**Authors:** Enrique Rojas Villalba, David Hysell

**Abstract:** Coherent radar backscatter from auroral E region irregularities can be measured with great precision and accuracy. The doppler data obtained from those measurements, coupled with empirical models, can provide a way to estimate convection patterns of the ionospheric plasma. These estimates show good correlations with optical and ISR data.

In the present work, we will first show some preliminary results of the comparison between all-sky images and convection patterns estimates from the event of December 20, 2015. We will also present some estimations of the spatial and temporal variability of electric field maps, calculated from the convection patterns, during active geomagnetic conditions and their relation to anomalous electron heating and global models.

## **ITIT-12 - Scientific Measurements Using Software Defined-Radio at MIT Haystack Observatory: Digital RF and it's Applications - by Bill Rideout**

Status of First Author: Non-student

**Authors:** Bill Rideout, Juha Vierinan, Frank Lind, Ryan Volz, and Phil Erickson

**Abstract:** MIT Haystack Observatory has leveraged software-defined radio to do scientific measurement for a number of years. These years of experiment have been leveraged to create a soon to be released open source product called Digital RF. Digital RF allows for the recording and storage of RF voltage data which allows for O(1) look up and reading for low level data. Along with it spiritual sibling project, Digital MetaData, this highly configurable software stack can help users to quickly deploy systems to do measurement. This new capability has opened up a large number of applications especially at the observatory. These include vector sensors, beacon receivers, antenna pattern measurement and future software architectures for large radar systems. Digital RF has also been used by students during workshops at Haystack and has shown promise to help open up the world radio science to a new generation.

## **ITIT-13 - Simulation of Particle Flow in Neutral Wind Sensor - by Ellen Robertson**

Status of First Author: Student IN poster competition Undergraduate

**Authors:** Robertson, Ellen; Earle, Gregory

**Abstract:** The Ram Energy Distribution Detector is a small satellite compatible neutral wind instrument. Simulations of the potential of and particle flow through the device direct the design of and corroborate testing of the instrument.

## **ITIT-14 - The Scintillation Prediction Observations Research Task (SPORT): Anticipated Data Products - by Jim Spann**

Status of First Author: Non-student PhD

**Authors:** James Spann<sup>1</sup>, Linda Krause<sup>1</sup>, Charles Swenson<sup>2</sup>, Rod Heelis<sup>5</sup>, Rebecca Bishop<sup>6</sup>, Guan Le<sup>7</sup>, Mangalathayil Abdu<sup>4</sup>, Otavio Durão<sup>3</sup>, Luis Loures<sup>4</sup>, Clezio Denardin<sup>3</sup>, Lidia Shibuya<sup>4</sup>, Joseph Casas<sup>1</sup>,



Shelia Nash-Stevenson<sup>1</sup>, Polinaya Muralikrishana<sup>3</sup>, Joaquim Costa<sup>3</sup>, Marcelo Banik de Padua<sup>3</sup>, Cristiano Wrasse<sup>3</sup>, and G. Fry<sup>1</sup>  
1 NASA/MSFC, 2 USU, 3 INPE, 4 ITA, 5 UTD, 6 Aerospace, 7 NASA/GSFC

**Abstract:** This poster presents analysis methods for studying the structuring and motion of ionospheric irregularities at the sub-kilometer scale sizes that produce L-band scintillations. A closely-spaced Global Navigation Satellite System (GNSS) receiver array has been established in the auroral zone at Poker Flat Research Range, Alaska for routine scintillation monitoring. Using the spaced-receiver technique historically applied to VHF signals, the correlation of the received phase signals are examined to estimate the following properties of the ground diffraction pattern: plasma drift velocity, diffraction anisotropy magnitude and orientation, and characteristic velocity. Uncertainties on estimates are quantified by ensemble simulation of noise on the phase signals carried through to the observations of the spaced-receiver linear system and then to uncertainties on drifts through linearization. A case study of multiple scintillating satellites observed by the array during a geomagnetic storm day is used to demonstrate the spaced-receiver and uncertainty estimation process. These scintillations are correlated with auroral activity, based on all-sky camera images. Measurements and uncertainty estimates made over a 30-minute period are made and compared to a collocated incoherent scatter radar, and show good agreement in horizontal drift speed and direction during periods of scintillation.

### **ITIT-15 - Resolution Metrics for Auroral Multipoint Measurements with Satellite Swarms - by Jonathan Parham**

Status of First Author: Student IN poster competition Masters

**Authors:** J. Brent Parham, Joshua Semeter

**Abstract:** With the growing accessibility of low cost satellite measurements, Boston University set out to create a space-based swarm called ANDESITE to do multipoint magnetometer measurements of the auroral current systems. In this work, we develop a model of the system and a rigorous, physically consistent, method to test its capability. With this methodology, any formation geometries can be evaluated for their ability to resolve postulated plasma wave phenomena that are superimposed onto the field aligned currents in the aurora. These investigations then inform the current design and future mission concepts that could help decipher energy transport in the magnetospheric-ionospheric coupling that occurs at high latitude.

### **ITIT-16 - Fitting Ionospheric Models Using Real-Time High Frequency Amateur Radio Observations - by Joshua Katz**

Status of First Author: Student IN poster competition Undergraduate

**Authors:** N.A. Frissell, A.J. Gerrard

**Abstract:** Empirical ionospheric models such as the International Reference Ionosphere (IRI) typically provide reliable monthly average characterizations of the global ionosphere but fail to adequately capture short-term variability. A relatively new source of large-scale ionospheric data is provided by amateur radio projects such as the Reverse Beacon Network (RBN), PSKReporter, and the Weak Signal Propagation Reporting Network (WSPRNet). These voluntarily operated networks automatically monitor, record, and report in real-time HF and VHF radio propagation links based on signals generated by routine amateur radio communications. Using the IRI and the PHARLaP ionospheric ray tracing toolkit, we report on the consistency of routine IRI runs to observations generated by the amateur radio networks and then propose an approach for fitting the IRI to these observations.

## **ITIT-17 - Preliminary Results from LITES and Model Comparison – by George Geddes**

Status of First Author: Student IN poster competition PhD

**Authors:** George Geddes, Susanna Finn, Andrew Stephan, Timothy Cook, and Supriya Chakrabarti

**Abstract:** The Limb-Imaging Thermosphere and Ionosphere EUV Spectrograph (LITES) is an instrument currently observing Extreme Ultraviolet (EUV) airglow from 600 - 1400 Å on the limb from the International Space Station. This range captures a number of EUV airglow features in the day and night. Data are shown and compared to model results from MSIS, IRI, and AURIC. These results show a proof of concept for LITES ionospheric measurements. Relative variations of emission features with latitude are also shown.

## **ITIT-18 - Particle-in-cell simulations of collisional ISR spectra - by William Longley**

Status of First Author: Student IN poster competition Masters

**Authors:** Meers Oppenheim, Alex Fletcher, and Yakov Dimant

**Abstract:** Incoherent scatter radars (ISR) reflect radio signals off the ionosphere and measure the returning wave spectra. These spectra are inverted with theoretical models to calculate the density and temperature of the electrons and ions, and the plasma flow speed. When the ISR beam points nearly perpendicular to the Earth's magnetic field, electron-ion Coulomb collisions significantly change the shape of the resulting spectra. This paper describes a grid-based Coulomb collision algorithm in the Electrostatic Parallel Particle-in-Cell (EPPIC) simulator. We simulate ISR spectra with and without electron-ion collisions. The results are compared to theoretical spectra for angles ranging from perpendicular to the magnetic field to 10 degrees from perpendicular. The results perpendicular to the magnetic field show narrower and more powerful spectra than collisionless theory predicts.

## **ITIT-19 - Thermospheric Measurements With Sounding Rocket Chemical Release Payloads - by Carl Andersen**

Status of First Author: Student IN poster competition Masters

**Authors:** Mark Conde

**Abstract:** Sounding rocket payloads capable of deploying multi-point chemical releases provide a unique tool for investigating several properties of the lower thermosphere. This type of payload consists of a collection of sub-payloads that are propelled laterally out of the rocket during flight, each containing a canister of liquid tracer which is dispersed by explosive detonation. The result is a luminous "puff" that can be tracked by triangulation using images taken from several ground stations and can yield measurements of the neutral winds and both turbulent and molecular diffusion near the turbopause.

## **ITIT-20 - Auroral energy and energy flux derivation using multi-spectral imaging – by Saurav Aryal**

Status of First Author: Student IN poster competition PhD

**Authors:** Saurav Aryal<sup>1</sup>, Kuravi Hewawasam<sup>1</sup>, Ryan Maguire<sup>1</sup>, Susanna C. Finn<sup>1</sup>, George Geddes<sup>1</sup>, Timothy Cook<sup>1</sup>, Jason Martell<sup>1</sup>, Jeffrey L Baumgardner<sup>2</sup> and Supriya Chakrabarti<sup>1</sup>

(1) University of Massachusetts Lowell, Lowell, MA, United States, (2) Boston University, Boston, MA, United States

**Abstract:** The aurora triggered by the June 22-23, 2015 G4 storm was observed using the High Throughput and Multi-slit Imaging Spectrograph (HiT&MIS) instrument from Lowell, MA. The field of view of HiT&MIS is  $0.1^\circ \times 50^\circ$  and measurements in the four above mentioned features were made simultaneously of OI (557.7 nm), OI (630.0 nm), OI (777.4 nm) and N<sub>2</sub><sup>+</sup> (427.8 nm) emission features at a cadence of one minute. The Ne I (630.5 nm) emission feature (also observed by HiT&MIS) was used as a tracer for cloud activity, and the appropriate times were picked for analysis based on its brightness.

Using the GLObal airGLOW (GLOW) model, the emission brightnesses were modeled for different input energies and energy fluxes of the precipitating electrons. The energy and energy fluxes for the observed aurora were then derived by using a chi-square minimization technique applied to the measured and modeled values. The derived energy values range between 100-200 eV suggesting a low energy precipitation event; and, the flux derived range from 1 to 2 erg cm<sup>2</sup> s<sup>-1</sup>.

This work was supported by NSF Grant AGS-1145166, ONR grant N00014-13-1-0266 and internal UMass Lowell funds.

### **ITIT-21 - Geophysical Inversion of thermospheric winds at 250km altitude using higher order Tikhonov regularization on the Alaskan Allsky Fabry-Pert interferometry network for the night of Jan 31st, 2016. - by John Elliott**

Status of First Author: Student IN poster competition PhD

**Authors:** John Elliott, Mark Conde

**Abstract:** Thermospheric winds were inverted using a higher order Tikhonov based method. Zeroth order regularization was performed and additionally a higher order "trust" regularization was added. The trust regularization is an axial summation of the absolute values of the geometric design matrix. This provides a metric per reconstructed cell of how much information was collected about that cell in the data. Results show improved reconstruction of winds, in accordance with other known methods.

### **ITIT-22 - The Design and Function of the Gridded Retarding Ion Distribution Sensor - by Anthony Swenson**

Status of First Author: Student IN poster competition Masters

**Authors:** Anthony Swenson, Dr. Ryan Davidson, Billy Hatch, Jordan Luke, and Bron McCall

**Abstract:** MIT Haystack Observatory has leveraged software-defined radio to do scientific measurement for a number of years. These years of experiment have been leveraged to create a soon to be released open source product called Digital RF. Digital RF allows for the recording and storage of RF voltage data which allows for O(1) look up and reading for low level data. Along with its spiritual sibling project, Digital MetaData, this highly configurable software stack can help users to quickly deploy systems to do measurement.

This new capability has opened up a large number of applications especially at the observatory. These include vector sensors, beacon receivers, antenna pattern measurement and future software architectures for large radar systems. Digital RF has also been used by students during workshops at Haystack and has shown promise to help open up the world radio science to a new generation.

## **ITIT-23 - Investigating Near Space Interaction Regions: Developing a Remote Observatory - by Margaret Gallant**

Status of First Author: Student IN poster competition Masters

**Authors:** Margaret Gallant, Edwin Mierkiewicz, Ronald Oliverson, Kurt Jaehnig, Jeff Percival, John Harlander, Christoph Englert, Robert Kallio, Fred Roesler, Susan Nossal, Derek Gardner, and Sara Rosborough

**Abstract:** The Investigating Near Space Interaction Regions (INSpIRE) effort will (1) establish an adaptable research station capable of contributing to terrestrial and planetary aeronomy; (2) integrate two state-of-the-art second generation Fabry-Perot (FP) and Spatial Heterodyne Spectrometers (SHS) into a remotely operable configuration; (3) deploy this instrumentation to a clear-air site, establishing a stable, well-calibrated observatory; (4) embark on a series of observations designed to contribute to three major areas of geocoronal research: geocoronal physics, structure/coupling, and variability. This poster describes the development of the INSpIRE remote observatory. Based at EmbryRiddle Aeronautical University (ERAU), initiative INSpIRE provides a platform to encourage the next generation of researchers to apply knowledge gained in the classroom to real-world science and engineering. Students at ERAU contribute to the INSpIRE effort's hardware and software needs. Mechanical/optical systems are in design to bring light to any of four instruments. Control software is in development to allow remote users to control everything from dome and optical system operations to calibration and data collection. In April 2016, we also installed and tested our first science instrument in the INSpIRE trailer, the Redline DASH Demonstration Instrument (REDDI). REDDI uses Doppler Asymmetric Spatial Heterodyne (DASH) spectroscopy, and its deployment as part of INSpIRE is a collaborative research effort between the Naval Research Lab, St. Cloud State University, and ERAU. Similar to a stepped Michelson device, REDDI measures oxygen (630.0 nm) winds from the thermosphere. REDDI is currently mounted in a temporary location under INSpIRE's main siderostat until its entrance optical system can be modified. First light tests produced good signal-to-noise fringes in ten minute integrations, indicating that we will soon be able to measure thermospheric winds from our Daytona Beach testing site. Future work will involve installation and software integration of FP and SHS systems and the EmbryRiddle Instrument Control System. The INSpIRE project is funded through NSF CAREER award AGS135231 and the NASA Planetary Solar System Observations Program. The REDDI instrument was supported by the Chief of Naval Research.

## **ITIT-24 - Monte-Carlo simulations of ion velocity distributions and resulting incoherent radar spectra under strong ion frictional heating conditions – by Lindsay Goodwin**

Status of First Author: Student IN poster competition Masters

**Authors:** L. V. Goodwin, J.-P. St.-Maurice, H. Akbari, and R. Spiteri

**Abstract:** In the presence of strong electric fields the ion velocity distribution of the weakly ionized plasma at high latitudes can differ enough from a Maxwellian shape to substantially affect Incoherent Scatter Radar (ISR) spectra, and thus the analysis and interpretation of those spectra. In the present work, an advanced description of the ion velocity distribution and attendant spectra is obtained through improvements made to previous studies that employed Monte-Carlo simulations. These improvements include: 1) a high precision one-dimensional ion velocity distribution, 2) a new velocity distribution fitting technique, 3) the use of Nyquist diagrams to check the plasma stability, 4) a study of more recently published O<sup>+</sup>-O resonant charge exchange collision cross-sections, 5) the option to incorporate the effects of ion-ion and ion-electron collisions on the ion velocity distribution, and 6) an improved filtering technique to reduce the statistical noise produced by the Monte Carlo simulations. Through these improvements, it has been found that: 1) ion-ion and ion-electron collisions have a minimal impact on the NO<sup>+</sup> line-of-sight temperature, but a strong impact on the O<sup>+</sup> temperature parallel to the magnetic field; 2) the newer O<sup>+</sup>-O resonant charge exchange collision cross-section published by Pesnell (1993) affects the results for the ion temperature

along a line-of-sight by several 1000 K under strong electric field conditions, as well as produces an electrostatically stable plasma, contrary to what is produced by the older Knoff et al. (1964) cross-section or the 'scaled' relaxation collision model that has frequently been used in the past; 3) NO<sup>+</sup> spectra can generally be modeled using Maxwellian velocity distributions as far as the impact on ISR spectra is concerned; and 4) O<sup>+</sup> spectra obtained along the magnetic field direction lead to an apparent increase in electron temperature, in contrast with the well-known opposite situation at large angles to the magnetic field.

### **ITIT-25 - Development of a commercial off-the-shelf software defined radio ionosonde - by Lee Kordella**

Status of First Author: Student IN poster competition PhD

**Authors:** L. Kordella, G.D. Earle, W. Loyd, D.G. Sweeney, R.W. McGwier, M. Moses, and X. Han

**Abstract:** Ionosondes (also known as chirpsounders) are a specialized application of HF radar for ionospheric diagnostics. By transmitting a frequency swept chirp waveform and measuring time of arrival of the received ionospheric reflected signal we can construct plasma density profiles of the ionosphere. The scientific merit of these diagnostics are achieved because the critical frequency of the plasma directly corresponds to the vertical penetration of the radio signal into the ionosphere. The key geophysical parameter of plasma density is then recovered as it is proportional to the square of the transmitted carrier frequency. The global map of ionosondes is relatively sparse primarily due to the cost of traditionally implemented systems. Here we present the development of a commercial off-the-shelf (COTS) software defined radio (SDR) ionosonde as an inexpensive and easily reproducible solution with the aim of bolstering our ionospheric monitoring networks.

## **INSTRUMENTS OR TECHNIQUES FOR MIDDLE ATMOSPHERE OBSERVATIONS**

### **ITMA-01 - Lower Atmosphere Ionosphere Coupling Experiment - by Channing Philbrick**

Status of First Author: Student IN poster competition Undergraduate

**Authors:** Channing Philbrick, Gary Swenson, and Greg Earle

**Abstract:** The LAICE satellite will be the first Earth satellite to exclusively investigate the energy and momentum transfer of waves produced by low-atmosphere weather systems to the mesosphere, lower thermosphere, and ionosphere. Built into a 6U CubeSat, LAICE will be compliant with NASA ELaNa launch standards and procedures. The LAICE CubeSat will be launched into a near circular orbit between 350 and 400 km, depending on International Space Station altitude at the time of release. The desired mission duration is approximately nine months in order to provide adequate longitudinal and local time coverage over three different seasons.

### **ITMA-02 - Toward a new capability for upper atmospheric research using atomic oxygen lidar - by James Clemmons**

Status of First Author: Non-student PhD

**Authors:** J. H. Clemmons, P. Steinvurzel, X. Mu, S. M. Beck, W. T. Lotshaw, T. S. Rose, J. H. Hecht, K. R. Westberg, M. F. Larsen, X. Chu, and D. Fritts

**Abstract:** Progress on development of a lidar system for probing the upper atmosphere based on atomic oxygen resonance is presented and discussed. The promise of a fully-developed atomic oxygen lidar system, which must be based in space to measure the upper atmosphere, for yielding comprehensive new insights is discussed in terms of its potential to deliver global, height-resolved measurements of winds, temperature, and density at a high cadence. An overview of the system is given, and its measurement principles are described, including its use of 1) a two-photon transition to keep the optical depth low; 2) laser tuning to provide the Doppler information needed to measure winds; and 3) laser tuning to provide a Boltzmann temperature measurement. The current development status is presented with a focus on what has been done to demonstrate capability in the laboratory and its evolution to a funded sounding rocket investigation designed to make measurements of three-dimensional turbulence in the upper mesosphere and lower thermosphere.

### **ITMA-03 - LWPC Modeling of Ionospheric Perturbations Due to Lightning Induced Energetic Electron Precipitation Using Overlapping VLF Propagation Paths - by Chad Renick**

Status of First Author: Student IN poster competition Undergraduate

**Authors:** Chad Renick, Mark Golkowski, Sandeep Sarker, and M. B. Cohen

**Abstract:** Lightning discharges are known to be a source of high amplitude, broad frequency electromagnetic radiation. These electromagnetic waves can cause perturbations in the electron density of the D-region of the ionosphere either by ionization from quasi-electrostatic fields or from induced energetic electron precipitation from the magnetosphere. The effect of these variations is more pronounced at nighttime due to nighttime electron densities being much lower when compared to daytime levels. Because changes in D-region electron density affect the conductivity of the ionosphere, nighttime lightning discharges can perturb the amplitude and phase of VLF communication signals propagating through the Earth-ionosphere waveguide. Most past work in this area has involved unique propagation paths between a transmitter and receiver. Modeling of such perturbation events often involves uncertainty since the perturbed ionospheric profile cannot be uniquely determined. In this work we focus on overlapping VLF propagation paths when signals from two different VLF transmitters share a common path to a receiver. This allows for the geographic area of the overlapping path to be simultaneously diagnosed with two signals with different mode content. Observations show that a lightning induced perturbation on the overlapping path can have a large effect on the amplitude or phase of one signal, while leaving the other wave relatively unaffected. The Long Wave Prediction Capability (LWPC) software package is used to simulate this phenomenon by altering the effective conducting height of the ionosphere near the location of a known nighttime lightning strike. Good agreement is found between the simulation and the observations providing additional constraints on the perturbed ionosphere and a more accurate model of how lightning affects ionospheric electron densities. Analyzing the mode structure of the propagating wave through LWPC simulation has led to a more complete understanding of why ionospheric disturbances often have different effects on individual VLF waves traveling on similar paths.

### **ITMA-04 - Detection and characterization of Turbulence with Incoherent Scatter Radar - by Jintai Li**

Status of First Author: Student NOT in poster competition Masters

**Authors:** J Li, R Collins, D Thorsen, and R. Varney

**Abstract:** Poster presents techniques for the detection and characterization of turbulence in the mesosphere using Incoherent Scatter Radar. Poster will discuss implications for understanding turbulence.

## **ITMA-05 - Observability of Acoustic Waves in the MLT by Ground-Based and Airborne Synthetic Airglow Imagers - by Jaime Aguilar Guerrero**

Status of First Author: Student IN poster competition PhD

**Authors:** Jaime Aguilar Guerrero, Jonathan B. Snively

**Abstract:** Acoustic wave (AWs) signals have recently been predicted to be detectable by imaging systems looking at OH airglow layer perturbations [Snively, GRL, 40, 2013 and Pilger et. al., JASP, 104, 2013]. These signals may be produced by AW generated from localized transient forcing in the troposphere or at the surface, such as due to storms or tsunamis. Indeed, recent observations via SABER following the Tohoku earthquake reported by Yang et. al. [GRL, 44, 2017] suggest that tsunami-generated gravity waves were detectable in the OH airglow layer above the ocean disturbance. However, while acoustic signatures were clearly identified in ionospheric total electron content (TEC) measured data over the same event [e.g., Zettergren et al., JGR, 122, 2017, and references therein], no instruments were present to unambiguously detect them in the MLT region, due in part to challenges related to the transient and short-lived nature of the waves along with their short periods. Detection of AWs will greatly depend on the imager (or photometer or spectrometer) being able to measure directly above the source, since wave amplitudes decay significantly with radial distance [e.g. Snively, 2013].

Recent imaging systems have sufficient spatial and temporal resolution to detect low frequency AWs with 1~5 min periods [Pautet et. al., AO, 53, 2014], and the detectability of the AWs (regardless of source) will be directly dependent on its location within the FOV of the imaging system. Previous efforts to show such feasibility have been limited to Cartesian integrations in a flat-Earth geometry [e.g. Snively, 2013] that are not able to account for line-of-sight (LOS) enhancements or cancellations due to oblique imaging angles as well as the related filtering of scales. In this study we employ a synthetic “airglow imager” framework that incorporates 2D and 3D modeled emission rate data and performs the necessary LOS integrations for synthetic imaging from ground-based or a moving platforms (e.g., airplanes or satellites). We use modeled acoustic and gravity wave perturbations to the hydroxyl layer from a nonlinear, compressible model [e.g., Snively et al., JGR, 115, 2010] for different case studies of ideally-generated AWs [e.g., Snively, 2013] and, more realistically, from the 2011 Tohoku-Oki earthquake ocean surface disturbance that subsequently led to the tsunami [Zettergren et al., 2017]. Using synthetic data, we identify preferable viewing angles and geometries for imaging of AWs above their sources. These simulations show some promise for the unambiguous determination of AWs in new and existing imager data. Furthermore, the synthetic data framework developed for this study allows for applications to other imaging systems from ground or space, or as applicable to other regions of the atmosphere.

## **LONG-TERM VARIATIONS OF THE MESOSPHERE AND LOWER THERMOSPHERE**

### **LTVM-01 - Zonal winds in the tropical middle atmosphere - by Anne Smith**

Status of First Author: Non-student PhD

**Authors:** Anne K. Smith, Rolando R. Garcia, Andrew C. Moss, and Nicholas J. Mitchell

**Abstract:** Zonal winds in the equatorial middle atmosphere from the middle stratosphere to the upper mesosphere vary on a semiannual time scale. The structure and variability of this Semi-Annual Oscillation (SAO) have not been well constrained by wind measurements and therefore not much is known about the processes that drive it. Here we use the balance wind relationship to derive monthly and zonally averaged zonal winds in the tropics from satellite retrievals of geopotential height from Aura/MLS and TIMED/SABER. The derived winds show prominent easterly maxima near the solstices at 1.0 hPa,

westerly maxima near the equinoxes at 0.1 hPa, and easterly maxima near the equinoxes at 0.01 hPa. The pressure and timing of the wind minima and maxima are variable from year to year. For all seasons except NH winter, the SAO winds in the mesosphere vary with the phase of the QBO in the middle stratosphere. During easterly QBO, the westerly maxima are shifted upward, are about 10 m s<sup>-1</sup> stronger, and occur approximately one month later than those during the westerly QBO phase.

### **LTVM-02 - Interannual Variations of SABER CO<sub>2</sub> and CO<sub>2</sub>-based Eddy Diffusion Coefficients in the Mesosphere and Lower Thermosphere Region – by Cornelius Csar Jude Salinas**

Status of First Author: Student IN poster competition PhD

**Authors:** Loren Chang, Mao-chang Liang, Jia Yue, Liying Qian, James Russel III and Martin Mlynczak

**Abstract:** The residual circulation in the mesosphere and lower thermosphere region (MLT region) is known to be controlled by breaking gravity waves. Observing this circulation and the gravity waves behind it is known to be difficult. Recently though, tracer species observations have allowed us to understand their seasonal variations. This work builds on these past works by exploring now their interannual variations. This work specifically uses SABER CO<sub>2</sub> profiles and SABER CO<sub>2</sub>-based Eddy Diffusion Coefficients to understand the interannual variations of the residual circulation and gravity wave forcing and mixing in the global MLT region. CO<sub>2</sub> is chemically inert and is known to be solely controlled by large-scale advection, eddy diffusion and molecular diffusion in the MLT region. Thus, it is an ideal tracer for such dynamics. First, composite analysis will be done on SABER global-mean and zonal-mean CO<sub>2</sub> profiles from 2002 to 2016 to try and isolate signatures by the Quasi-biennial Oscillation (QBO) and the El Nino Southern Oscillation (ENSO). The same analysis will also be applied to SABER global-mean eddy diffusion coefficients. Then, the same analysis will be applied to outputs from the Specified Dynamics – Whole Atmosphere Community Climate Model (SD-WACCM) for comparison to assess how well SD-WACCM reproduces these observations and also to understand the physics behind the QBO and ENSO in the MLT region.

## **METEOR SCIENCE OTHER THAN WIND OBSERVATIONS**

### **METR-01 - A Simulation of Plasma Turbulence from Dust Gradients. - by Matthew Young**

Status of First Author: Student IN poster competition PhD

**Authors:** Matthew A. Young, Meers M. Oppenheim

**Abstract:** This work presents simulations of gradient-driven plasma turbulence in the vicinity of a static layer of charged dust in Earth's ionosphere. Dust layers formed by ablated meteors are present in the altitude range corresponding to the upper mesosphere/lower thermosphere, or upper D/lower E regions of the ionosphere. Typical dust grains are many orders of magnitude more massive than the surrounding ions and neutrals, and may therefore be treated as static on the timescales of plasma dynamics. Dust layers become charged via attachment of electrons, creating a depletion in electron density that the plasma cannot replenish if it is to maintain quasineutrality in the absence of appreciable creation or loss. The result is an overall gradient in mobile charge carriers in the vicinity of a dust layer. Such gradients create instabilities that ground-based radars measure, providing a diagnostic for dust density, dynamics, and lifetime. Previous studies provide the theoretical foundation for studying static, ionized dust layers at 80--100 km in Earth's atmosphere, and observations have attributed radar echoes associated with ice grains in the polar mesosphere to charged dust. A recently developed hybrid particle/fluid numerical model of the weakly ionized plasma found in Earth's lower ionosphere is well suited for simulations of dust--plasma



interactions. Preliminary simulations with a simple 2--D dust model exhibit plasma turbulence perpendicular to the ambient magnetic field that can be understood as a modified form of the gradient-drift instability.

### **METR-02 - Effect of Plasma Turbulence on the evolution of Specular Meteor Echoes - by Freddy Galindo**

Status of First Author: Student NOT in poster competition PhD

**Authors:** Julio Urbina, Lars Dyrud, and Jonathan Fentzke

**Abstract:** Specular meteor echoes are signals back-scattered from expanding trails of ionized particles created during the passage of a meteoroid through the upper atmosphere, when a radar k vector points perpendicularly to the trajectory of the trail. These radar echoes are currently used to derive atmospheric parameters such as temperature, pressure, and drifts; under the assumption of non-turbulent diffusion rate. In this paper, we describe a numerical model of under-dense specular meteor echoes that includes for the first time the effect of plasma turbulence on its evolution. In other words, this simulator incorporates the studies of diffusion values, which are modeled by including/excluding the effect of the Earth's geomagnetic field and plasma turbulence. Our numerical method simulates both the trail at different stages and its corresponding received power. This numerical model can easily be expanded to include physical processes (e.g. differential ablation) that briefly affect the evolution of the specular meteor echo.

We present the analysis of a specular meteor echo that exhibit a double decay as a case study. Our simulations demonstrate that meteor events similar to this double decay can occur when time-scales to produce plasma turbulence in the trail is on the order of hundreds of milliseconds, or when plasma turbulence ceases rapidly. Furthermore, we report a statistical analysis that combine our numerical model of under-dense specular meteor echoes with the meteor input function in order to investigate the importance of plasma instabilities in the meteor population detected by all-sky radars. Upon examination of simulations and experimental data, our preliminary studies illustrate the significant effect that turbulence plays on the evolution of underdense specular meteor echoes. This result is particularly useful to infer more accurate mesospheric temperatures from trail diffusion rates and their usage for meteor scatter communication systems.

### **METR-03 - PIC Simulations of 3D Finite Meteor Trails - by Liane Tarnecki**

Status of First Author: Student NOT in poster competition Undergraduate

**Authors:** Liane Tarnecki, Meers Oppenheim

**Abstract:** Presents simulation results and spectra of finite meteor trail segments.

## **MLT GRAVITY WAVES**

### **MLTG-01 - Selection of an atmospheric reference model and branching ratios for numerical modeling of gravity wave-airglow interactions - by Yolian Amaro-Rivera**

Status of First Author: Student IN poster competition PhD

**Authors:** Dr. Tai-Yin Huang, Dr. Julio Urbina

**Abstract:** Airglow emissions depend on the number density of the light-emitting species, so it is important to select an atmospheric reference model that accurately represents the initial state of the atmosphere in numerical studies for gravity wave-airglow interactions. Previous simulation results using chemistry dynamics numerical models show that the airglow emissions magnitude, shape, and wave-induced response also vary with different branching ratios. We assess the effect of the atmospheric reference model in numerical studies and conduct a virtual experiment to investigate the Volume Emission Rates (VER) of O(1S) greenline and O<sub>2</sub>(0,0) atmospheric band when using different branching ratios for their productions. The branching ratio, alpha, is the leading determining factor for the O(1S) VER production whereas the branching ratios, epsilon and alpha, determine the O<sub>2</sub> atmospheric band VER production. Using a numerical optimization approach, we match the simulated VERs to VERs from observations to determine optimal branching ratios. We present and discuss the results of our 2-dimensional, nonlinear, time-dependent numerical models, Multiple Airglow Chemistry Dynamics (MACD) and OH Chemistry Dynamics (OHCD) when using different atmospheric reference models and the computed branching ratios.

### **MLTG-02 - Application of the Transfer Function Model (TFM) in gravity wave modeling - by Robert Bruntz**

Status of First Author: Non-student PhD

**Authors:** Robert Bruntz, Hans Mayr, and Larry Paxton

**Abstract:** The Transfer Function Model (TFM) is a linear model that solves the equations for the conservation of mass, energy, and momentum in the atmosphere, from 0 to 700 km, for 5 species (N<sub>2</sub>, O, H, He, Ar) and 4 parameters for each (density + 3 components of velocity), plus the (same) temperature for all species. TFM is unusual in that rather than solving the equations and obtaining results on a fixed grid, the response to a delta-function source is saved in an intermediate-state transfer function, which can be combined with any number of different sources in a separate step, producing the atmospheric response on a user-defined grid of arbitrary resolution in time and colatitude. The model uses zonally-symmetric sources (cylinders at the pole or pole-centered rings), which can then be linearly combined to simulate complicated sources. We will present results from several applications of the TFM, using a variety of sources in the thermosphere and lower atmosphere.

### **MLTG-03 - Measurements of phase differences between temperature and vertical wind perturbations associated with gravity waves in the mesopause region - by Anthony Caton**

Status of First Author: Student IN poster competition Undergraduate

**Authors:** Anthony Caton, Fabio Vargas, and Gary Swenson

**Abstract:** The study of the phasing of gravity wave temperature and vertical wind perturbations ( $T'$  and  $W'$ ) in the mesopause region dates to 2003, when Swenson et al. used correlative measurements of temperature and vertical wind from Na lidar and airglow brightness (OH and O<sub>2</sub>) to show a relation between gravity wave damping and the phase difference between  $T'$  and  $W'$  parameters. The measurements enable studies of wave state, i.e. freely propagating or damped. Data from the Andes Lidar Observatory (ALO) on Cerro Pachon, Chile (30.25° S, 70.74° W) Na wind/temperature lidar are sufficient to resolve gravity wave  $T'/W'$  phase differences with altitude. Phase data from two nights are presented along with  $T'$ ,  $W'$ , and convective instability data for each night to provide a more comprehensive picture of the gravity wave effects.

### **MLTG-04 - Multi-Scale Gravity Wave Environments and Influences on Gravity Wave Propagation - by Katrina Bossert**

Status of First Author: Non-student PhD

**Authors:** Katrina Bossert, Dave Fritts, Tyler Mixa, Dominique Pautet, Mike Taylor, and Bifford Williams

**Abstract:** Multi-scale gravity wave environments, including those with smaller vertical scales (<7 km) have the potential to influence gravity wave propagation and momentum deposition in the mesosphere and lower thermosphere. These environments can have especially strong influences for small-horizontal wavelength gravity waves by producing critical levels, ducting regions, and regions that can destabilize the gravity wave and induce breaking. This poster investigates a multi-scale gravity wave environment observed over ALOMAR (69N, 16E) in Norway, and the ability for varying scales of gravity waves to modulate the background environment. Different wave spectra are isolated from the background as well as associated upward and downward propagating gravity waves. The impacts of the different spectra are discussed as well as the potential for different scales of gravity waves to be influenced by the particular environment.

### **MLTG-05 - GPS TEC Detection of MSTIDs/LSTIDs and Source Determination – by Ross Dinsmore**

Status of First Author: Student IN poster competition Undergraduate

**Authors:** Dinsmore, Ross, Mathews, John

**Abstract:** GPS total electron content (TEC) data allows for a horizontal resolution not possible with singular radar/optical systems. Incoherent scatter radar (ISR) data of medium/large scale traveling ionospheric disturbance (MSTID/LSTID) events are correlated to GPS TEC results of the same event. The GPS TEC large horizontal ranging then allows for those same MSTID/LSTID events' sources to be determined.

### **MLTG-06 - Classifying mesospheric mountain wave characteristics over New Zealand during the 2014 DEEPWAVE campaign – by Pattilyn McLaughlin**

Status of First Author: Student NOT in poster competition PhD

**Authors:** Pattilyn McLaughlin, Mike Taylor, Dominique Pautet, Bernd Kaifler, Steve Smith, and Yucheng Zhao

**Abstract:** The Deep Propagating Gravity Wave Experiment, “DEEPWAVE” was a highly successful international measurement and modelling program designed to characterize the generation and propagation of a broad range of atmospheric gravity waves (GWs) with measurements extending from the ground to ~100 km altitude. These waves typically arise from sources located at lower altitudes such as storms, frontal weather systems, and winds interacting with mountain ranges. They dissipate at high altitudes in the Mesosphere-Lower Thermosphere (MLT) region (~80-100km) depositing large amounts of momentum. A suite of aircraft-borne and ground-based aeronomic and weather measurements was deployed from New Zealand during a two-month period (June-July) in 2014 to investigate the wintertime gravity wave climatology.

In this study we utilize data obtained by a collection of ground-based instrumentation operated at NIWA Lauder Station, NZ (45.0°S). Instruments included an Advanced Mesospheric Temperature Mapper (AMTM), a Rayleigh Lidar and an All-Sky Imager. An initial analysis of image data obtained by the AMTM showed a rich spectrum of GWs. An astounding 19 events were identified as signatures of mesospheric Mountain Waves (MW) generated by orographic forcing. This is by far the largest outflowing of MW activity ever recorded at MLT heights. The observed events were quasi-stationary, exhibited a variety of horizontal wavelengths and lasted for a few to several hours.

This poster presents an overview of 4 of the 19 observed MW events, focusing on the evolution of their characteristics, and associated breaking patterns. The results of this study are crucial as they will impact our current knowledge and understanding of MW penetration to high altitudes.

**MLTG-07 - Multi-Year Survey of Short Period Gravity Wave Parameters in the Mesosphere and Lower Thermosphere at McMurdo (77.8°S, 166.7°E), Antarctica - by Ian Geraghty**

Status of First Author: Student IN poster competition Undergraduate

**Authors:** Ian Geraghty, Xinzhao Chu, Jian Zhao, and Cao Chen

**Abstract:** Recent observations made by the University of Colorado Lidar group using an Fe Boltzmann lidar reveal that temperature variations in the Antarctic Mesosphere/ Lower Thermosphere are driven by seemingly ever present, short period gravity waves. Waves with periods of ~3 – 10 hours and vertical wavelengths of ~20 – 30 km have been present and dominant in the upper atmosphere temperature perturbations for every lidar run over multiple years of observation. Internal gravity waves play a key role in distributing energy and momentum throughout the atmosphere and so an understanding of any seasonal changes in their properties is necessary to fully understand the dynamics of the MLT region. In order to characterize seasonal variations of these gravity waves, a two-dimensional fast Fourier transform is used to analyze the period and vertical wavelength spectra of multiple years of temperature and Fe density measurements. Emphasis is placed data collected during the Antarctic winter months because of an abundance of long-duration lidar observations with high signal to noise ratios. While sources of these waves remain unknown, we hope that clues as to possible sources arise through this analysis and comparison with gravity wave trends at lower altitudes.

**MLTG-08 - Automated estimation of dominant horizontal wave parameters appearing in airglow images - by Matthew Grawe**

Status of First Author: Student IN poster competition Masters

**Authors:** Matthew Grawe, Jonathan Makela

**Abstract:** It is well known through both observation and theory that internal gravity waves generate signatures in the 630.0-nm airglow. The horizontal properties of these signatures (e.g., wavelength, phase speed, period, orientation) are useful to measure as they provide information about the characteristics of the internal gravity wave. Here, we present a technique that automatically estimates (potentially in real-time) the parameters of the dominant wave features appearing in data from airglow imaging systems. We show results of the technique applied to several sets of imaging data.

**MLTG-09 - Rayleigh/Raman lidar observations of gravity wave activity in the middle atmosphere over Syowa (69°S, 40°E), Antarctic – by Masaru Kogure**

Status of First Author: Student IN poster competition PhD

**Authors:** Masaru Kogure, Takuji Nakamura, Mitsumu K. Ejiri, Takanori Nishiyama, Yoshihiro Tomikaw, and Masaki Tsutsumi

**Abstract:** The potential energy of gravity waves (GWs) per unit mass ( $E_p$ ) in the middle atmosphere has been examined from temperature profiles obtained by our Rayleigh/Raman (RR) lidar at Syowa Station (69°S, 40°E) from May 2011 to October 2013, with the exception of the summer months. The GWs with ground-based wave periods longer than 2 h and vertical wavelengths between 1.8 and 16 km were extracted

from the temperature profiles.  $E_p$  was the largest in winter, although in 2012, at altitudes below 30 km,  $E_p$  was the largest in spring.  $E_p$  increased with a mean scale height of 11.3 km.  $E_p$  profiles showed a local maximum at an altitude of 20 km and a minimum at 25 km in almost every month, which has not been reported by previous studies observed by radiosondes. The values of  $E_p$  in October of 2012 were smaller at 35–60 km and larger at 20–35 km than those in October of 2011 and 2013. This difference in the  $E_p$  profile is most probably caused by different seasonal variations of zonal winds. The larger and smaller  $E_p$  values seem to be observed both below and above the altitude at which the zonal wind speed reached 0 m s<sup>-1</sup>. This result suggests that wind filtering of gravity waves with small phase speeds is significantly important in early spring.

## **MLTG-10 - Coupling by gravity waves through the middle and upper atmosphere in Antarctica: Are dominant stratospheric gravity waves the direct source of persistent gravity waves in the MLT? - by Jian Zhao**

Status of First Author: Student IN poster competition PhD

**Authors:** Jian Zhao, Xinzhao Chu, Sharon L. Vadas, Erich Becker, Cao Chen, Xian Lu, Michael R. Jones, and Andreas Dörnbrack

**Abstract:** Persistent gravity waves with periods of 3–10 h and vertical wavelengths of 20–30 km were discovered in the Mesosphere and Lower Thermosphere (MLT) above McMurdo, Antarctica from Fe Boltzmann lidar observations [Chen et al., 2013, 2016; Chen and Chu, 2017]. Several theories have been proposed for the sources of these waves, e.g., resonant vibration of Ross ice shelf [Godin and Zabolin, 2016] and secondary wave generation [Vadas et al., 2003; Vadas and Becker, private communication, 2017]. Chen et al. [2013] performed a ray-tracing study and pointed possible wave sources to the stratosphere. Furthermore, gravity waves are found to play crucial roles in the formation of thermospheric Fe layers and such waves are traced down to the stratosphere [Chu et al., 2011; Chu and Yu, 2017]. All these discoveries urge the need to analyze gravity waves in the stratosphere to shed light on the sources of gravity waves in the MLT.

We characterized the lognormal distributions of vertical wavelengths, periods, vertical phase speeds, and potential energy densities from atmospheric temperature observations (30 to 50 km, year 2011 to 2015) obtained by the Fe Boltzmann lidar. Over 1000 dominant gravity wave events are identified. The fractions of gravity waves with downward phase progression increase from summer ~59% to winter ~70%. The monthly mean vertical wavelengths and periods exhibit clear seasonal cycles with vertical wavelength growing from summer ~5.5 km to winter ~8.5 km, and period increasing from summer ~4.5 h to winter ~6 h. Statistically significant linear correlations are found between the monthly mean vertical wavelengths/periods and the mean zonal wind velocities from 30–50 km given by ECMWF. Assuming horizontal phase speeds constant through a year, the monthly mean horizontal wavelengths, intrinsic periods, and group velocities are inferred for stratospheric gravity waves. In general, gravity waves propagate along north-south direction with elevation angles  $\sim 1.1^\circ$  and horizontal phase speeds  $\sim 20$  m/s. The horizontal wavelengths of gravity waves in the stratosphere vary from 350 to 450 km, which are much shorter than those of the persistent waves in the MLT (at least 1000 km to over 2000 km). We conclude that the dominant gravity waves in the stratosphere are not the direct source of the persistent gravity waves in the MLT.

Secondary wave generation theory provides the explanation for the source of such persistent gravity waves. Primary waves generated from the lower atmosphere tend to break at  $\sim 50$  km and create body forces, which lead to the generation of secondary gravity waves. These secondary gravity waves are speculated to provide the persistent waves that we observed in the MLT above McMurdo Station. “Fish-bone” patterns in the temperature perturbations, which are the theoretically predicted patterns from the secondary wave generation theory by Vadas and Becker, will be presented from our lidar measurements.

## MLTL LIDAR STUDIES

### **MLTL-01 - Investigation of Na layer by numeric simulation - by Xuguang Cai**

Status of First Author: Student IN poster competition PhD

**Authors:** Xuguang Cai, Tao Yuan, Vince Eccles

**Abstract:** In this poster, we build a Na model and conduct numerical simulations of the mid-latitude lower E region where both the ion density and the neutral atmosphere are modulated by tidal waves and gravity waves. We found that, based on the current Na ion-molecular theory in the literature, it is highly difficult for the Na neutralization to occur within the Es above 100 km. The simulation shows that, while the Na chemistry mainly works to decrease the density of Na, the vertical winds perturbations induced by strong tidal and/or gravity waves play a critical role in modulating Na density through converging the Na atoms into layer structure at high altitudes. The eddy diffusion in the lower E region can also have dramatic effects on the spatial structure and temporal variations of the Na density.

### **MLTL-02 - Depletion of mesospheric sodium during extended period of pulsating aurora: high speed sodium lidar observation - by Toru Takahashi**

Status of First Author: Non-student PhD

**Authors:** Toru Takahashi, Keisuke Hosokawa, Satonori Nozawa, Takuo T. Tsuda, Yasunobu Ogawa, Masaki Tsutsumi, Yasutaka Hiraki, Hitoshi Fujiwara, Takuya D. Kawahara, Norihito Saito, Satoshi Wada, Tetsuya Kawabata, Chris Hall, and Hiroshi Miyaoka

**Abstract:** In the last three decades, the impact of auroral particle precipitation on the neutral Na layer has been studied at high latitudes. Recently, we employed simultaneous observations by the sodium lidar and the European Incoherent Scatter (EISCAT) VHF radar at Tromsø, Norway (69.6°N, 19.2°E), to study the effect of auroral particle precipitation on Na density. Our simultaneous observations clearly showed an occurrence of Na density depletion during auroral ionization. The depletion around 100 km reached up to ~60% of the nightly mean Na density. However, it was still unclear which of the suggested mechanisms dominated the observed Na density depletion.

In this study, we quantitatively evaluated the Na density depletion due to charge transfer reactions between Na atoms and molecular ions produced by high-energy electron precipitation during a pulsating aurora (PsA). An extended period of PsA was captured by an all-sky camera at the EISCAT radar site during a 2-h interval from 00:00 to 02:00 UT on 25 January 2012. During this period, using the EISCAT VHF radar, we detected three intervals of intense ionization below 100 km that were probably caused by precipitation of high-energy electrons during the PsA. In these intervals, the sodium lidar at Tromsø observed characteristic depletion of Na density at altitudes between 97 and 100 km. These Na density depletions lasted for 8 min and represented 5-8% of the background Na layer. To examine the cause of this depletion, we modeled the depletion rate based on charge transfer reactions with NO<sup>+</sup> and O<sub>2</sub><sup>+</sup> while changing the R value which is defined as the ratio of NO<sup>+</sup> to O<sub>2</sub><sup>+</sup> densities, from 1 to 10. The correlation coefficients between observed and modeled Na density depletion calculated with typical value R=3 for time intervals T1, T2, and T3 were 0.66, 0.80 and 0.67.

This good agreement suggests that the charge transfer reactions triggered by the auroral impact ionization at low altitudes is the predominant process responsible for Na density depletion during PsA intervals. In this presentation, we will present about these results in detail and future plans for this study by using an upgrade in the data recording and laser control system for the Tromsø sodium lidar.

### **MLTL-03 - Simultaneous Lidar Measurements of Fe and Na layers, Temperatures, and Winds in the Mesosphere and Lower Thermosphere-Extended (MLT-X) at Boulder, Colorado - by Dongming Chang**

Status of First Author: Student IN poster competition PhD

**Authors:** Dongming Chang, Xinzhao Chu, Jian Zhao, Cao Chen, John A. Smith, Runnan Lou, Zhengyu Hua, et al.

**Abstract:** Previous work at McMurdo, Antarctica [Chu et al., 2011, 2012, 2013] demonstrated that thermospheric neutral Fe layers were observed to 170 km or higher, and the measured elevated temperatures appeared to be associated with the Joule heating enhanced by aurora. Following the McMurdo work, more observations of metal layers extended into the middle thermosphere have been reported, mainly in the polar region and in the equatorial region. A detailed study by Huang et al. [2013] from 12 nights of observations at Boulder, Colorado derived the correlation between Fe/Na densities and temperatures in the mesosphere and lower thermosphere (MLT) with an Fe Boltzmann lidar and a Na Doppler lidar. However, the Boulder observations in 2010 were mainly made in September without yearly coverage. Also at that time the signal levels from both lidars were quite low (~10-30 counts per shot), not allowing comprehensive investigation of Fe and Na layers into the MLT-extended region at such a mid-latitude site.

Now two powerful resonance-Doppler lidars (namely the Fe and Na Doppler lidars) have been developed at the University of Colorado Boulder with signal levels ranging from ~100 to 2000 counts per shot. These two lidars have been operated at the Table Mountain Lidar Observatory near Boulder to acquire yearly observations in the MLT-X region. In this paper we provide the first study of simultaneous and common-volume observations of Fe density, Na density, and their seasonal variations for the entire year with the Fe and Na Doppler lidars in Boulder. We also report the first comparisons of the temperatures and vertical winds acquired by the Fe and Na Doppler lidars in the MLT-X region. Such simultaneous and common-volume lidar observations provide unique opportunities to study how Fe and Na layers respond to various physical, dynamical and chemical processes and to evaluate the most advanced Doppler lidars for temperature and wind measurements.

### **MLTL-04 - Na lidar measurements of turbulence heat flux, thermal diffusivity and energy dissipation rate in the mesopause region - by Yafang Guo**

Status of First Author: Student NOT in poster competition PhD

**Authors:** Alan Z. Liu, Chester S. Gardner

**Abstract:** Turbulence is ubiquitous in the mesopause region, where the atmospheric stability is low and wave breaking is frequent. Measuring turbulence is challenging in this region and is traditionally done by rocket soundings and radars. In this work, we show for the first time that the modern Na wind/temperature lidar located at Andes Lidar Observatory in Cerro Pachón, Chile is able to directly measure the turbulence perturbations in temperature and vertical wind between 85 and 100 km. Using 150 h of lidar observations, we derived the frequency ( $\omega$ ) and vertical wavenumber ( $m$ ) spectra for both gravity wave and turbulence, which follow the power law with slopes consistent with theoretical models. The calculated turbulence heat flux and energy dissipation result in a net cooling of  $-4.9 \pm 1.5$  K/d, comparable to that due to gravity wave transport at  $-7.9 \pm 1.9$  K/d. The derived mean turbulence thermal diffusivity and energy dissipation rate are  $43 \text{ m}^2/\text{s}$  and  $37 \text{ mW/kg}$  in the mesopause region, respectively. Turbulence key parameters show consistency with turbulence theories.

### **MLTL-05 - Initial Results of Na Lidar Measured Stratospheric Temperatures at Andes Lidar Observatory (30.3°S, 70.7°W) - by Shuai Qiao**

Status of First Author: Student IN poster competition PhD

**Authors:** Shuai Qiao, Alan Liu, Weilin Pan, and Yafang Guo

**Abstract:** We derived Rayleigh temperature from Na lidar measurement made at the Andes Lidar Observatory in Chile. The initial results of Rayleigh temperature profiles were compared with the MSIS-00 (Mass Spectrometer and Incoherent Scatter) model and SABER temperature between 30~50 km. The results show that nightly mean temperature profiles can be derived between 30 km to 70 km and hourly mean temperature profiles can be derived between 30 km to 50 km, with maximum error less than 10K. This work will enrich the stratospheric temperature dataset, and enable the study of gravity wave propagation from the stratosphere to the mesopause at ALO. Some caveats of using Na lidar to calculate Rayleigh temperature are also discussed.

## MESOSPHERE OR LOWER THERMOSPHERE GENERAL STUDIES

### **MLTS-01 - Statistical Characteristics of Short-term Tidal Variability for DW1 in eCMAM30 and SABER - by Ashan Vitharana**

Status of First Author: Student IN poster competition Masters

**Authors:** Ashan Vitharana<sup>1</sup>, Jian Du<sup>1</sup>, Jens Oberheide<sup>2</sup>, and William E. Ward<sup>3</sup>

Department of Physics and Astronomy, University of Louisville, Louisville, KY, USA

Department of Physics, Clemson University, Clemson, SC, USA

Department of Physics, University of New Brunswick, Fredericton, NB, CANADA

**Abstract:** In this research, we compare the statistical characteristics of DW1 (migrating diurnal tide) short-term variability using data from the extended Canadian Middle Atmosphere Model (eCMAM30) run (1979-2010) and the Sounding of the Atmosphere using Broadband Emission Radiometry (SABER) instrument on NASA's TIMED (Thermosphere Ionosphere Mesosphere Energetics Dynamics) satellite. SABER short-term tides are diagnosed with the deconvolution method (Oberheide et al., 2002). Both eCMAM30 and SABER DW1 time series (variability on the order of 5 days) are first fitted to a multiple linear regression model with deterministic inter-annual variability predictors such as ENSO, QBO, Solar Flux (monthly mean values are used for these indices) and 12, 6, 4, 3 months seasonal harmonics. The residue of the time series is further separated into undeterministic long-term variation (> 1 month) and short-term variation (< 1 month). Characteristics of the above predictors, their relative variance, cross-correlations and probability density functions (PDFs) of the short-term tidal variability (< 1 month) were investigated and compared between the two datasets. Many of the statistical properties agree very well between the two datasets. The model should be able to provide some explanations of the physical processes underlying these statistical properties, which is part of our future research.

### **MLTS-02 - Validation of NASA TIMED/SABER v2.0 temperature data with ground-based lidars: first results. - by Erin Dawkins**

Status of First Author: Non-student PhD

**Authors:** E.C.M. Dawkins<sup>(1,2)</sup>, A.A. Kutepov<sup>(1,2)</sup>, A. Feofilov<sup>(3)</sup>, L. Rezac<sup>(4)</sup>, and D. Janches<sup>(1)</sup>

1. NASA Goddard Space Flight Center, Greenbelt, MD, USA

2. Catholic University of America, Washington, DC, USA

3. Department of Planets and Comets, Max-Planck-Institut für Sonnensystemforschung, Justus-von-Liebig-Weg 3, 37077 Göttingen, Germany.

4. Laboratoire de Météorologie Dynamique, IPSL/CNRS, UMR8539, Ecole Polytechnique, Paris, France.



**Abstract:** The mesosphere/lower thermosphere region (75-110 km) is very sensitive to temperature perturbations, with temperature signatures being easier to detect here than in the lower atmosphere, where the diurnal temperature variation is much larger than the warming over the past 150 years [Plane et al., 2015]. It is imperative to continue to both accurately monitor these temperatures, and maintain consistent and well-calibrated instrumental temperature records, in order to better understand the nature of this temperature variability on a variety of timescales.

The NASA Thermosphere Ionosphere Mesosphere Energetics and Dynamics (TIMED) Sounding of the Atmosphere using Broadband Radiometry (SABER) instrument is a 10-channel broadband limb-scanning infrared radiometer which covers the spectral range 1.27-17  $\mu\text{m}$ . Launched in December 2001, SABER performs near-global measurements which provides information on the vertical kinetic temperature profiles and volume mixing ratios of various trace species (including O<sub>3</sub>, CO<sub>2</sub> and H<sub>2</sub>O), with data available from 2002 to present. In this work, we use the SABER v2.0 operational retrieval algorithm product, which uses a combination of the measured 15  $\mu\text{m}$  CO<sub>2</sub> vertical emission profile and a CO<sub>2</sub> vertical mixing ratio as calculated by the National Center for Atmospheric Research (NCAR) Whole Atmosphere Community Climate Model (WACCM).

We performed a comparative study of the co-located SABER v2.0 multi-year average kinetic temperature profiles with those from three different northern hemisphere lidar station locations; Arecibo (18oN, 293oE), Logan (42oN, 112oE), and ALOMAR (69oN, 16oE). We compared multi-year seasonal averages in an effort to assess the performance of the SABER v2.0 product relative to the high-resolution lidar temperature profiles. We found differences between the SABER v2.0 and lidar temperature profiles, which varied with season and latitude. In this work, we seek to better understand and examine the nature of these differences, as a means for further improving this important SABER dataset.

### **MLTS-03 - Nonlinear acoustic wave effects on lower thermosphere composition - by Benedict Pineyro**

Status of First Author: Student IN poster competition Masters

**Authors:** Benedict Pineyro, Jonathan B. Snively

**Abstract:** Small-scale dynamical models for the diffusive and stratified lower thermosphere [e.g. Snively and Pasko, JGR, 113, 2008] commonly use single gas approximations with height-dependent physical properties (e.g. mean molecular weight, specific heats) that do not vary with time (fixed composition). This approximation is useful as it is simpler and less computationally expensive than a true multi-constituent fluid model, and still captures the important physical transitions between molecular and atomic gases in the lower thermosphere. However, during extreme disturbances, such as the 2011 Tohoku earthquake, nonlinear acoustic waves or shocks may strongly modulate the composition of the lower thermosphere [e.g., Zettergren et al., JGR, 122, 2017]. Models with composition-dependent gas properties have been shown to outperform commonly used models with fixed properties [Walterscheid and Hickey, 2001, JGR, 106]. Time-dependent compositional effects may be included in a one-gas model by adding a conservation equation for the molecular weight, leading to better agreement with a true binary-gas model [Walterscheid and Hickey, JGR, 117, 2012].

This paper presents a one-dimensional nonlinear mass fraction approach to multi-constituent gas modeling on a similar premise as Walterscheid and Hickey [2001, 2012] (e.g. less computationally intensive than a full binary-gas model). Our approach uses the finite volume method of Bale et al. [SIAM JSC, 24, 2002] implemented in Clawpack [<http://www.clawpack.org>; LeVeque, 2002] with a Riemann Solver to solve the Euler Equations including multiple species, defined by their mass fractions, as they undergo advection. To validate this method, tests are conducted including shock tube problems for a two-species gas, vertically propagating acoustic waves with oscillations near the cut-off frequency, and propagating nonlinear acoustic waves with steep or pseudo-shock character. The limits of applicability of model assumptions are also investigated.

## **MLTS-04 - Mesospheric temperatures during day and night estimated from meteor radar observation - by Jeong-Han Kim**

Status of First Author: Non-student PhD

**Authors:** Jeong-Han Kim, Changsup Lee, Geonhwa Jee, and Yong Ha Kim

**Abstract:** We have been operating VHF meteor radar at King Sejong Station (62S, 58W), Antarctica, since its installation on 2007, in order to measure neutral winds and temperatures in polar mesosphere region. The KSS meteor radar operating at 33.2 MHz with the peak power of 12 kW shows high-performance that detects the meteor echoes of about 15,000 ~ 40,000 per day with maximum in summer and minimum in winter. In this study, we provide the day- and night-time mesospheric temperatures estimated from KSS meteor radar observations with the new method that uses full width at half maximum (FWHM) in meteor height distribution. In addition, we compare the results with the temperatures measured from MLS instrument onboard on Aura satellite and discuss about the difference between two temperatures and the variability of the estimated mesospheric temperatures.

## **MLTS-05 - Seasonal Variation of Ozone in the Upper Mesosphere at High Latitudes - by Nabil Nowak**

Status of First Author: Student IN poster competition PhD

**Authors:** Nabil Nowak, Brentha Thurairajah, and Scott M. Bailey

**Abstract:** Ozone in the upper mesosphere and lower thermosphere (55-105 km) has been measured by The Solar Occultation for Ice Experiment (SOFIE) instrument on the Aeronomy of Ice in the Mesosphere (AIM) satellite. The ozone measurements at  $.292 \mu\text{m}$  were made over 9 years (2007-2016) in the latitude range of  $65^\circ$ - $85^\circ$  in both hemispheres at a high vertical resolution (1.8 km). In the upper mesosphere (85~95 km), large seasonal variation can be noticed where the ozone mixing ratio observed at the winter solstice is 3-4 times higher than summer solstice. What controls this seasonal variation of ozone is still up for much debate. These variations are annual in nature and occur every year in both hemispheres. The characteristics of the variations also change with altitude. In this study we use water vapor, also measured by SOFIE and atomic oxygen inferred from ozone measurements to understand the cause of the observed variability in ozone. Preliminary analysis indicates that the driving force for the seasonal variation of ozone is the variability of atomic oxygen and water vapor in the upper mesosphere, with ozone positively correlated with atomic oxygen and negatively correlated with water vapor.

## **MLTS-06 - New method of estimating temperatures near the mesopause region using meteor radar observations - by Changsup Lee**

Status of First Author: Non-student PhD

**Authors:** Changsup Lee, Jeong-Han Kim, Geonhwa Jee, Wonseok Lee, In-Sun Song, and Yong Ha Kim

**Abstract:** We present a novel method of estimating temperatures near the mesopause region using meteor radar observations. While previous method using meteor decay times requires priori information such as temperature gradient, the new method simply utilizes the linear relationship between the width of the meteor height distribution and the temperature near the meteor peak height. The temperatures estimated from the FWHM are consistent with the Aura-MLS temperatures throughout the study period within a margin of 3.0%. TIMED-SABER temperatures providing better vertical resolution than MLS are also used to find a specific height region of temperature derived from FWHM. In this study, we suggest the exact proportionality constant in linear relationship between FWHM and temperature from experimental and theoretical bases.

**MLTS-07 - Comparison Between Thermospheric Nitric Oxide Emission Observations and the Global Ionosphere-Thermosphere Model (GITM) Simulations: Sensitivity Study to Solar and Geomagnetic Activities - by Cissi Lin**

Status of First Author: Non-student PhD

**Authors:** Cissi Y. Lin, Yue Deng, Karthik Venkataramani, Justin Yonker, and Scott Bailey

**Abstract:** Nitric oxide (NO), a minor species in the thermosphere, is an important indicator of energy balance in the upper atmosphere because its production comes from energy sources able to break the strong bond of molecular nitrogen. It displays as a big challenge to the community to precisely estimate energy budget (heating and cooling) in the ionosphere and thermosphere especially during geophysical events. Works in the recent decades have significantly improved our understanding of NO chemistry and its relationship to energy, such as the role of the excited state of nitrogen, N<sub>2</sub>(A), in the thermospheric NO reactions. In this study, the chemical scheme is updated in the Global Ionosphere Thermosphere Model (GITM) to study NO density, emission, and temperature responses in the lower thermosphere to the solar and geomagnetic activities. Particularly, we investigate the sensitivity of the 5.3- $\mu$ m NO emission to F10.7 and Ap indices by comparing the global integrated emission from GITM with an empirical proxy from the Sounding of the Atmosphere using Broadband Emission Radiometry (SABER) measurements. GITM's output total emission shows solar and geomagnetic dependency and agrees well within  $\pm 20\%$  of the empirical values. Localized enhancement of  $\sim 70\%$  in column density and 3 times in column emission are observed in a moderate storm case study. The altitudinal zonal mean emission agrees well with observations during storm time.

**MLTS-08 - Simulations of MLT dynamics with global circulation models and their comparison with mid- and high-latitude ground-based radar observations - by Dimitry Pokhotelov**

Status of First Author: Non-student PhD

**Authors:** Dimitry Pokhotelov, Gunter Stober, Erich Becker, and Jorge L. Chau

**Abstract:** Multi-year observations of mesospheric neutral winds in 80-100 km altitude range obtained using ground-based radars in Northern Germany (55 deg N) and Northern Norway (69 deg N) will be presented. Contribution of tides into the observed wind spectrum is separated from the mean flow / planetary waves and from the contribution of gravity waves. Observational results are compared to the global simulations of tidal spectrum using Kuelungsborn Mechanistic Circulation Model. Seasonal variability of tidal magnitudes and their possible connection to the spectrum of gravity waves will be analyzed. The results will be discussed in connection to the simulations of tides with the Whole Atmosphere Community Climate Model.

**MLTS-09 - New non-LTE model of OH(v) in the mesosphere/lower thermosphere - by Peter Panka**

Status of First Author: Student NOT in poster competition Masters

**Authors:** Peter Panka, Alexander Kutepov, Konstantinos Kalogerakis, Diego Janches, Artem Feofilov, Ladi Rezac, Daniel Marsh, and Erdal Yigit

**Abstract:** We present a new detailed non-LTE model of OH(v) for the nighttime mesosphere/lower thermosphere. The model accounts for chemical production of vibrationally excited OH and for various

vibrational-vibrational (VV) and vibrational-translational (VT) energy exchanges with main atmospheric constituents. The new feature was added to account for the "indirect" vibrational-electronic (VE) mechanism  $\text{OH}(v) \rightarrow \text{O}(1D) \rightarrow \text{N}_2(v)$  of the OH vibrational energy transfer to N<sub>2</sub>, recently suggested by Sharma et al. [2015] and confirmed through laboratory studies by Kalogerakis et al. [2016]. We study the impact of this mechanism on the OH(v) populations and emissions in the two SABER channels at 1.6 and 2.0  $\mu\text{m}$ . We also discuss the implications this mechanism will have on the retrieval of OH and O densities, as well as its effects on the nighttime CO<sub>2</sub> density retrievals from the SABER 4.3  $\mu\text{m}$  channel.

## **MLTS-10 - OPAL CubeSatellite Data Analysis Model - by Kenneth Zia**

Status of First Author: Student NOT in poster competition Masters

**Authors:** Kenneth Zia, Ludger Scherliess, Michael J. Taylor, and the OPAL Team

**Abstract:** Understanding the Earth's lower thermosphere (altitude range 90km-140km) is of growing interest for many areas of research within the space weather community. The NSF-sponsored OPAL (Optical Profiling of the Atmospheric Limb) mission is designed to measure the thermospheric temperature profile from 90 to 140 km by observing the integrated daytime line of sight O<sub>2</sub> A-band (~760nm) emissions on the limb. The OPAL instrument has an altitude resolution of about 1km and is expected to be launched from the International Space Station (ISS) (~400km altitude). We have used a model of OPAL's position and attitude of its optical system to investigate the instrument's ability to detect space weather signatures (i.e. solar storms and gravity waves) in the lower thermosphere temperature. Models of the flight, line-of-sight, and atmospheric O<sub>2</sub> A-band emission are used to simulate the expected observations of the OPAL instrument. The simulated emissions are used together with an inversion method to obtain the altitudinal temperature profile in the lower thermosphere. This data will be used to test our ability to spatially and temporally resolve variability in the lower thermospheric temperatures.

## MLTT OTHER TIDAL, PWS, OR SSWS

### **MLTT-01 - Seasonal and solar cycle variability of DE2 and DE3 in the CO<sub>2</sub> 15 $\mu\text{m}$ cooling of the lower thermosphere - by Nirmal Nischal**

Status of First Author: Student IN poster competition Masters

**Authors:** Jens Oberheide, Martin Mlynczak, Linda Hunt, and Astrid Maute

**Abstract:** In this paper we demonstrate that upward propagating nonmigrating tides forced by latent heat release in the troposphere impact the thermospheric energy budget by modulating the longitudinal/local time behavior of the CO<sub>2</sub> infrared cooling of the lower thermosphere. Tidal diagnostics of SABER data shows that the CO<sub>2</sub> cooling rate amplitudes for the DE2 and DE3 components are on the order of ~20-50% relative to the zonal monthly means and their seasonal behavior closely follows the dynamical tides. The DE2 and DE3 in CO<sub>2</sub> cooling rates show a clear variability over a solar cycle owing to the variability in the temperature and atomic oxygen during that period. Supporting photochemical modeling reproduces the observed results, although with systematic amplitude differences which are related to the uncertainty in the model input backgrounds, especially atomic oxygen. The main tidal coupling mechanism below 110 km is temperature; however, neutral density becomes equally important above 110 km, thereby explaining observed evanescent DE2 and DE3 phases which are not present in the temperature tides. The contribution of vertical advection is comparatively small. The relative importance of the coupling mechanisms is largely independent of season and solar cycle.

## **MLTT-02 - Exploring Wave-Wave Interactions in a General Circulation Model - by Virginia Nystrom**

Status of First Author: Student NOT in poster competition Undergraduate

**Authors:** Virginia Nystrom, Federico Gasperini, Jeffrey M. Forbes and Maura E. Hagan

**Abstract:** Nonlinear wave-wave interactions are explored within a TIME-GCM simulation for April, 2009, forced at its ~30 km lower boundary by 3-hourly MERRA output. The main interacting (primary) waves are diurnal tides DW1, DW2, DE2, DE3 and two ultra-fast Kelvin waves, UFKW1 and UFKW2, with zonal wavenumber  $s = -1$  and respective periods of 3.7d and 2.4d. Model analysis identifies 12 significant secondary waves resulting from interactions between these primary waves. Another 5 secondary waves are interpreted as being due to interactions between DW1 and DW2, and  $s = 0$  and  $s = +1$  6-day and 9-day oscillations. In this poster, a few notable examples of temperature and wind amplitude and phase structures are presented and interpreted. The additional complexity imposed on the dynamics by the presence of the secondary waves are shown to be significant. Remaining questions to be addressed are articulated.

## **MLTT-03 - The quasi 2 day wave response in TIME-GCM nudged with NOGAPS-ALPHA - by Jack Wang**

Status of First Author: Student IN poster competition PhD

**Authors:** Jack C. Wang, Loren C. Chang, Jia Yue, Wenbin Wang, and D.E. Siskind

**Abstract:** The quasi 2 day wave (QTDW) is a traveling planetary wave that can be enhanced rapidly to large amplitudes in the mesosphere and lower thermosphere (MLT) region during the northern winter postsolstice period. In this study, we present five case studies of QTDW events during January and February 2005, 2006 and 2008–2010 by using the Thermosphere-Ionosphere-Mesosphere Electrodynamics-General Circulation Model (TIME-GCM) nudged with the Navy Operational Global Atmospheric Prediction System-Advanced Level Physics High Altitude (NOGAPS-ALPHA) Weather Forecast Model. With NOGAPS-ALPHA introducing more realistic lower atmospheric forcing in TIME-GCM, the QTDW events have successfully been reproduced in the TIME-GCM. The nudged TIME-GCM simulations show good agreement in zonal mean state with the NOGAPS-ALPHA 6 h reanalysis data and the horizontal wind model below the mesopause; however, it has large discrepancies in the tropics above the mesopause. The zonal mean zonal wind in the mesosphere has sharp vertical gradients in the nudged TIME-GCM. The results suggest that the parameterized gravity wave forcing may need to be retuned in the assimilative TIME-GCM.

## **MLTT-04 - A New Approach to Study Short-Term Nonmigrating Tidal Variability using Information Theory and Bayesian Statistics - by Komal Kumari**

Status of First Author: Student IN poster competition Masters

**Authors:** Komal Kumari, Jens Oberheide, and Jian Du-Cains

**Abstract:** Nonmigrating tidal diagnostics of SABER temperature observations in the mesosphere-lower thermosphere reveal a large amount of variability on time-scales of a few days to weeks. The physical reasons for the observed short-term variability are not well understood. In this poster, we present a new approach to diagnose how short-term tidal variability changes as a function of Madden-Julian Oscillation, QBO, solar cycle and others. Our approach is based on Information theory and Bayesian statistics using time dependent probability density functions, Shannon entropy and Kullback-Leibler divergence. The statistical significance of this approach is exemplified using SABER DE3 tidal diagnostics. The response of short-term DE3 variability to the QBO phase and other natural drivers will be discussed using principal component analysis of the time dependent probability density functions.

## SPRITES

### **SPRT-01 - Numerical and analytical studies of corona discharge initiation in air & CO<sub>2</sub>-rich environment - by Jacob Engle**

Status of First Author: Student IN poster competition Undergraduate

**Authors:** Jacob A. Engle; Jeremy A. Rioussset

**Abstract:** In this proposal, we focus on plasma discharge produced between two electrodes with a high potential difference, resulting in ionization of the neutral gas particles and creating a current in the gas medium. This process, when done at low current and low temperature can create corona and “glow” discharges, which can be observed as a luminescent, or “glow,” emission. The parallel plate geometry used in Paschen theory is particularly well suited to model experimental laboratory scenario. However, it is limited in its applicability to lightning rods and power lines. Franklin’s sharp tip and Moore et al.’s[6] rounded tip fundamentally differ in the radius of curvature of the upper end of the rod. Hence, we propose to expand the classic Cartesian geometry into spherical geometries. In a spherical case, a small radius effectively represents a sharp tip rod, while larger, centimeter-scale radius represents a rounded, or blunted tip. Experimental investigations of lightning-like discharge are limited in size. They are typically either a few meters in height, or span along the ground to allow the discharge to develop over a large distance. Yet, neither scenarios account for the change in pressure, which conditions the reduced electric field, and therefore hardly reproduce the condition of discharge as it would occur under normal atmospheric conditions.[2] In this work we explore the effects of shifting from the classical parallel plate analysis to spherical and cylindrical geometries more adapted for studies of lightning rods and power transmission lines, respectively. Utilizing Townsend’s equation for corona discharge, we estimate a critical radius and minimum breakdown voltage that allows ionization of neutral gas and formation of a glow corona around an electrode in air. Additionally, we explore the influence of the gas in which the discharge develops. We use Bolsig+, a numerical solver for the Boltzmann equation, to calculate Townsend coefficients for CO<sub>2</sub>-rich atmospheric conditions.[4] This allows us to explore the feasibility of a glow corona on other planetary bodies such as Mars. We calculate the breakdown criterion both numerically and analytically to present simplified formulae per each geometry and gas mixture.

### **SPRT-02 - Fractal properties of lightning from high-speed video observations - by Ningyu Liu**

Status of First Author: Non-student PhD

**Authors:** Ningyu Liu<sup>1</sup>, Julia Tilles<sup>1</sup>, Levi Boggs<sup>2</sup>, Alan Bozarth<sup>2</sup>, Jeremy Rioussset<sup>3</sup>, and Hamid Rassoul<sup>2</sup>

<sup>1</sup>Department of Physics and Space Science Center (EOS), The University of New Hampshire, Durham, NH, USA.

<sup>2</sup>Department of Physics and Space Sciences, Florida Institute of Technology, Melbourne, FL, USA.

<sup>3</sup>Center for Space and Atmospheric Research (CSAR), Physical Sciences Department, Embry Riddle Aeronautical University, Daytona Beach, FL, USA.

**Abstract:** The concept of fractals has been used to describe and understand complex development and spatial structure of lightning, jets, and sprites. In those transient electrical discharges, the discharge channels may branch repeatedly or extend with irregular paths, forming a discharge network beyond the ability of fluid or particle models. The modeling studies based on the fractal concept has achieved certain success, reproducing phenomenological properties of lightning [Mansell et al., JGR, 107, 4075, 2002; Rioussset et al., JGR, 112, D15203, 2007;], jets [Pasko and George, JGR, 107, 1458, 2002; Krehbiel et al.,

Nat. Geosci., 1, 233, 2008; Rioussset et al., JGR, 115, A00E10, 2010] and sprites [Pasko et al., GRL, 27, 497, 2000]. The fractal models used in those studies are all based on the stochastic growth approach proposed by Niemeyer et al. [PRL, 52, 1033, 1984] to model dielectric breakdown. There are several key parameters in the dielectric breakdown model of Niemeyer et al [1984], the values of which were determined by comparing the modeling results with laboratory electrical discharge experiments. Those values have never been rigorously validated for the natural discharges.

We conducted an observational campaign in the summer of 2016 to study lightning, jets, and sprites. A few interesting lightning discharges were recorded by a high-speed camera. The video recordings show that the propagation of lightning discharge channels is very complex, particularly for high-peak current lightning. The downward propagating lightning typically has multiple branches when it first enters the field of view of the camera, and each of them splits repeatedly during the subsequent propagation. In this talk, we present a detailed analysis of the high-speed images and formulate useful constraints to the fractal model of lightning.

## STRATOSPHERE STUDIES AND BELOW

### **STRB-01 - Analysis of Black carbon emissions over a semi-urban station Vijayawada: Preliminary results - by Prasad Perumal**

Status of First Author: Student IN poster competition Masters

**Authors:** P. Prasad<sup>1</sup>, M. Roja Raman<sup>1</sup>, Wei Nai Chen<sup>2</sup>, M. Venkat Ratnam<sup>3</sup>, and S. Vijaya Bhaskara Rao<sup>1\*</sup>

<sup>1</sup>Department of Physics, S.V.University, Tirupati – 517502

<sup>2</sup>RCEC, Academia Sinica, Taipei, Taiwan – 115

<sup>3</sup>National Atmospheric Research Laboratory, Gadanki, Tirupati - 517502

**Abstract:** Continuous measurements of Black Carbon (BC) aerosol mass concentration using multi wavelength advanced Aethalometer (AE-33) at Vijayawada (16.51°N 80.62°E), a semi-urban site in the southeast India, during January–December, 2016 has been analysed and presented in this study. The added advantage of the advanced aethalometer (AE-33) is to provide the estimates of percentage of Biomass Burning (BB) out of the total BC concentration directly. This helps to understand the contribution of anthropogenic activities to the observed BC concentrations. The diurnal and seasonal variation of BC concentrations and their relation to the back ground meteorological conditions have been investigated over this site for the first time. A significant diurnal variation in BC concentration is observed with two prominent peaks one in the morning hours ~0800-0900h IST (IST=UT+0530 h)) and the other in the evening around ~2100h IST. During mid afternoon hours around ~1400-1600h IST the BC concentration is seen minimum in all months. The maximum BC concentration is observed during November ( $6.88 \pm 0.47 \mu\text{g}/\text{m}^3$ ) and minimum during August ( $1.7 \pm 0.23 \mu\text{g}/\text{m}^3$ ) over this location. The seasonal mean BC mass concentration is high during Winter (DJF,  $4.68 \pm 1.32 \mu\text{g}/\text{m}^3$ ) and less during Summer monsoon (JJA,  $1.83 \pm 0.61 \mu\text{g}/\text{m}^3$ ). Whereas it is moderate during Pre-monsoon (MAM) and Post-monsoon (SON) seasons of about  $2.44 \pm 0.8 \mu\text{g}/\text{m}^3$ ,  $2.2 \pm 2.08 \mu\text{g}/\text{m}^3$  respectively. The higher BB(%) is observed during Pre-monsoon ( $25.21 \pm 7.02 \%$ ) and minimum in Summer monsoon ( $16.83 \pm 4.15 \%$ ). The mean Angstrom exponent ( $\alpha$ ) obtained during the period is ( $1.66 \pm 0.6$ ) indicates that the major contributor of BC over this location is biomass burning. The concentrated weighted trajectories (CWT) analysis performed for different seasons with 5day air mass back trajectories at an altitude of 500m reveals that the particles are advected from both land and oceanic regions to this site.

**Keywords:** Black Carbon, Biomass burning, Angstrom exponent, Aethalometer.

## **STRB-02 - Carbon dioxide in the polar stratosphere from AIM/SOFIE measurements - by Yucheng Su**

Status of First Author: Student IN poster competition Masters

**Authors:** Yucheng Su, Jia Yue, Mark Hervig, Tom Marshall, Anne Smith, Rolando Garcia, Dong Guo, Shengli Guo, David Siskind, and James Russell III

**Abstract:** The Gridded Retarding Ion Distribution Sensor (GRIDS) is a CubeSat-compatible instrument currently being designed at the Center for Space Engineering at Utah State University. GRIDS combines the functionality of a Retarding Potential Analyzer and an Ion Drift Meter into one small form factor suitable for small satellites. The sensor is capable of measuring the three-dimensional ion drift vector, ion density, and ion temperature when placed on a three-axis stabilized spacecraft with sufficient attitude control performance. An overview of the instrument is presented and a detailed description of the implementation of the command and control functions is given.



Aguilar Guerero, Jaime, 18  
 Amaro-Rivera, Yolian, 20  
 Andersen, Carl, 13  
 Aryal, Saurav, 13  
  
 Bossert, Katrina, 21  
 Bruntz, Robert, 21  
  
 Cai, Xuguang, 25  
 Caton, Anthony, 21  
 Chang, Dongming, 26  
 Chang, Loren, 7  
 Chiu, Shih-Chi, 5  
 Chou, Minyang, 1  
 Clemmons, James, 16  
  
 Dawkins, Erin, 27  
 Debchoudhury, Shantanab, 8  
 Dinsmore, Ross, 22  
 Duann, Yi, 8  
  
 Elliott, John, 14  
 Engle, Jacob, 33  
  
 Frissell, Nathaniel, 10  
 Fritz, Bruce, 9  
  
 Galindo, Freddy, 20  
 Gallant, Margaret, 15  
 Gan, Quan, 1  
 Geddes, George, 13  
 Geraghty, Ian, 23  
 Goodwin, Lindsay, 15  
 Grawe, Matthew, 23  
 Guo, Yafang, 26  
  
 Harding, Brian, 9  
  
 Inchin, Pavel, 3  
  
 Katz, Joshua, 12  
 Kim, Jeong-Han, 29  
 Kogure, Masaru, 23  
 Kordella, Lee, 16  
 Kumari, Komal, 32  
  
 Lee, Changsup, 29  
 Li, Jintai, 17  
 Lin, Cissi, 30  
 Liu, Ningyu, 33  
  
 Longley, William, 13  
  
 Malhotra, Garima, 1  
 Mao, Ya-Chih, 7  
 Maruyama, Naomi, 2  
 McGranaghan, Ryan, 6  
 McInerney, Joe, 4  
 McLaughlin, Pattilyn, 22  
 Moral, Aysegul, 4  
  
 Nischal, Nirmal, 31  
 Nowak, Nabil, 29  
 Nystrom, Virginia, 32  
  
 Panka, Peter, 30  
 Parham, Jonathan, 12  
 Perumal, Prasad, 34  
 Philbrick, Channing, 16  
 Pineyro, Benedict, 28  
 Pokhotelov, Dimitry, 30  
  
 Qiao, Shuai, 26  
  
 Renick, Chad, 17  
 Rideout, Bill, 11  
 Robertson, Ellen, 11  
 Rojas Villalba, Enrique, 11  
  
 Salinas, Cornelius Csar Jude, 19  
 Siddiqui, Tarique, 3  
 Sivadas, Nithin, 7  
 Smith, Anne, 18  
 Song, Huan, 10  
 Spann, Jim, 11  
 Su, Yucheng, 35  
 Swenson, Anthony, 14  
  
 Takahashi, Toru, 25  
 Tarnecki, Liane, 20  
  
 Vitharana, Ashan, 27  
  
 Wang, Jack, 32  
 Wu, Chen, 5  
 Wu, Qian, 3  
  
 Young, Matthew, 19  
  
 Zhao, Jian, 24  
 Zia, Kenneth, 31